Doctoral Thesis

An ADP-ribosyltransferase Alt of bacteriophage T4 negatively regulates the *Escherichia coli* MazF toxin of a toxin–antitoxin module

Abdulraheem Alawneh
Department of Biological Sciences, Graduate School of Science,
Osaka University

2016

Table of contents

An ADP-ribosyltransferase Alt of bacteriophage T4 negatively regulates the *Escherichia coli* MazF toxin of a toxin–antitoxin module

An ADP-ribosyltransferase Alt of bacteriophage T4 negatively regulates the *Escherichia coli* MazF toxin of a toxin–antitoxin module

PROLOGUE

Recently, our group identified a novel type II Toxin-Antitoxin system, RnlA-RnlB, and demonstrated that RnlAB is the essential component of RNase LS (*Ueno and Yonesaki, 2001; Otsuka and Yonesaki 2005; Koga et al., 2011*). RNase LS activity becomes much stronger after T4 infection and antagonizes T4 phage by degrading T4 late mRNAs preventing their expression. RnlAB is the first clear example of a TA system as an antiphage agent.

Although TA systems were speculated to act as antiphage agents, very little supporting evidence was provided so far and the molecular interaction between T4 phage and TA systems remains unclear. *E. coli* K-12 is predicted to possess at least 37 TA systems and like RnlA, most of the type II toxins have endoribonuclease activities *(Yamaguchi and Inouye, 2011; Wang et al., 2012).* Considering that the short-lived antitoxins must be constantly expressed to antagonize their cognate toxins and T4 infection immediately shuts off *E. coli* gene expression (*Kutter et al., 1994*), I suspect that other type II TA systems might function as anti-phage mechanisms and that T4 phages might encode antitoxins against *E. coli* toxins for their own survival.

In this study, I addressed the relationship between T4 infection and the two of the most characterized type II TA system, RelB-RelE and MazE-MazF.

An overview of phage-host arms race

Bacteria play crucial role in all ecosystems on the planet and although it is widely believed that bacteria are the most abundant organisms on earth, it is not entirely true simply due to the presence of bacteriophages. Bacteriophages, as the name implies, are viruses that nurture in their specific bacterial hosts. Until late 1970's, it was assumed that phages were present in relatively low numbers and that their effect on microbial communities was low (*Torrella F. and Morita RY., 1979*). However, with the increasing availability of new molecular techniques, it is now realized that phages greatly outnumber bacteria in their natural environments, with viral numbers (~10^7–10^8 ml^{-1}) often tenfold larger than bacterial cell counts (~10^6 ml^{-1}) (*Riesenfeld et al., 2004; Bergh et al 1989; Chibani-Chennoufi et al., 2004; Wommack et al., 2000*). Thus, bacteria are confronted with a constant threat of phage predation.

With such constant competitive environmental interaction, bacteria are forced to continuously adapt and acquire defense mechanisms against phages. On the other hand, phages must counter this host adaptation to keep their position as successful predators. This arms race affects all ecosystems on this planet and in the next few paragraphs I will briefly introduce some bacterial defense mechanisms and their phage counterparts.

A. Restriction-modification systems (degradation of foreign DNA):

Bacteria possess restriction-modification (RM) systems that allow recognition of foreign DNA. Those systems consist of two main components: one that restricts foreign DNA and the other protects self genetic material. Both restriction and protection activities are dependent on the recognition of a specific DNA sequence often 4-8 base pairs long. While restriction depends on DNases that recognize a specific DNA sequence then cleave it, protection is usually accomplished through DNA modification. Modification enzymes recognize the same sequence that the restriction enzymes recognize and modify it (usually methylation) thus the resulting modified DNA will no longer be

recognized by restriction enzymes making bacterial DNA immune against digestion by restriction enzymes.

Although RM is a very powerful strategy, phages have evolved to evade RM systems in a variety of ways. For example, some phages acquire Methyltransferases or stimulate the host Methyltransferases to modify the phage genome (*Kruger and Bickle, 1983*), other phages code for proteins that target and shut down the activity of host restriction enzymes (*Bandyopadhyay et al., 1985*), while some phages incorporate unusual bases in their genomes thus preventing restriction enzymes recognition of their DNA (*Kruger and Bickle, 1983; Wang and Mosbaugh 1988 & 1989*).

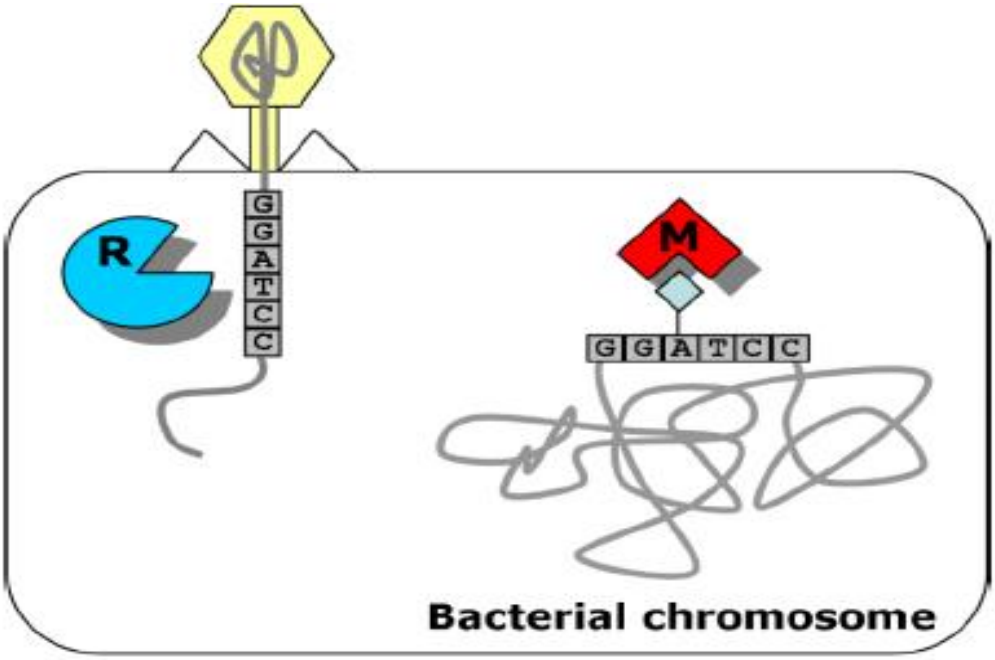

Schematic representation of RM systems immunity (adapted form Adi Stern and Rotem Sorek, 2011)

B. CRISPR/Cas systems (Adaptive immune systems):

CRISPR (Clustered Regularly Interspaced Short Palindromic Repeats) are unique DNA sequences comprised of a cluster of direct repeats interspersed with variable sequences termed spacers both around 30 bp long (*Ishino et al. 1987*). These clusters are found together with several CRISPR-associated (*cas*) genes, hence referred to CRISPR/Cas systems. After phage infection, a portion of the infected cells was found to have acquired new spacers identical to the infecting phage DNA. Those new spacers together with Cas proteins can then recognize and cleave the phage DNA (*Barrangou et al. 2007*). Thus CRISPR/Cas systems represent adaptive immune systems that can be inherited and interfere with foreign genetic material.

Although CRISPRs were reported in 1987 (*Ishino et al. 1987*), it was until 2007 that those systems were linked to phage immunity (*Barrangou et al. 2007*). While the study of CRISPR/Cas is still relatively new, phages that can escape CRISPR/Cas immunity were already reported. For instance, after the first round of infection and spacer acquisition by bacteria, some progeny phages mutated to actually lose their proto-spacer sequences rendering them resistant to CRISPR/Cas activity (*Barrangou et al. 2007; Deveau et al., 2008; Heidelberg et al., 2009*). Also, it is believed that some phages have evolved to directly target the CRISPR/Cas machinery. However, conclusive evidence is yet to be reported. For example, it has been shown that one of the proteins encoded by the T7 phage phosporylates the CasB protein (*Qimron et al., 2010*). It remains to be shown whether this feat of the phage affects CRISPR/Cas functioning.

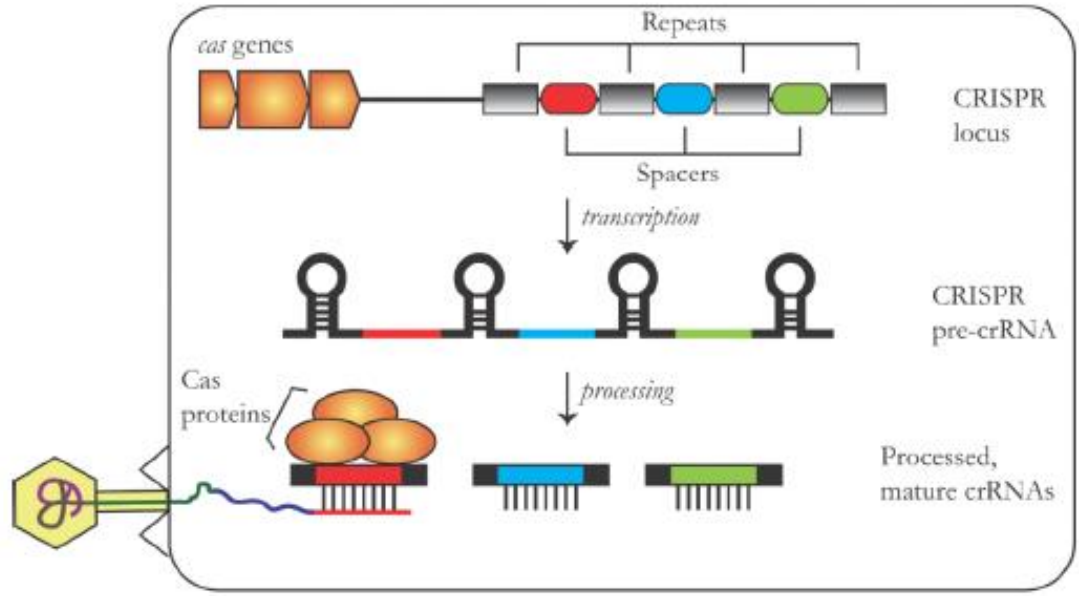

Schematic representation of CRISPR/Cas immunity (adapted form Adi Stern and Rotem Sorek, 2011)

C. Abortive infection (Cellular suicide):

Being under such constant predation pressure and constant evolutionary arms race, bacteria must ensure its survival by any means necessary. Thus, it is crucial to be ready for emergencies and in this case, abortive infection (Abi) comes to play. If a phage infects a cell and successfully escapes RM systems and CRISPR/Cas systems (and other defense systems), then the infected bacteria might choose to "self-destruct" as a last resort to prevent the spread of infectious particles to the rest of the population. Although several Abi systems have been found, the mechanism by which they operate remains largely unknown. Some Abi genes have been shown to target phage genes involved in DNA replication (*Durmaz and Klaenhammer, 2007; Bidnenko et al., 1995*) and others have been shown to target the host translation apparatus (*Georgiou et al., 1998; Morad et al., 1993*) For example, in *E. coli* K-12 the Lit protease, encoded by the defective e14 prophage, is activated only in the presence of a short polypeptide called Gol produced by the T4 phage. Activation of this protease cleaves the translation elongation factor Ef-Tu, thus leading to translational arrest

and cell death. However, phage mutants were found to escape the activation of Lit and propagate normally (*Georgiou et al., 1998)*. Although evidence is scarce, it is also believed that Toxin-Antitoxin systems are other examples of Abi systems.

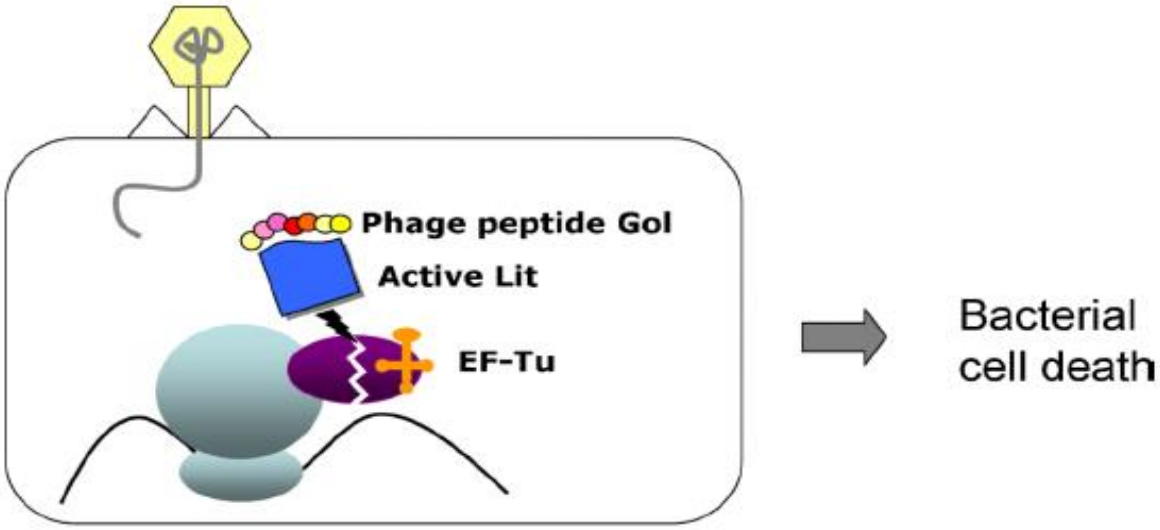

Schematic representation of Abi immunity by Lit (adapted form Adi Stern and Rotem Sorek, 2011)

All together, it is evident that bacteria have developed multi layered defense systems against phage infections and as soon as one of them is compromised the next will come to play all together forming a circle of protection. Unfortunately for bacteria, the circle is not perfect and phages often find their ways to crack it leaving us watching a non-ending evolutionary battle in which I believe there is no absolute winner.

Because my own study is focused on TA systems, next I briefly introduce an overview of TA systems.

An overview of Toxin-Antitoxin systems

Toxin-Antitoxin (TA) systems have been found on the genome of many bacteria and Archea (*Gerdes et al., 2005*). To date, six types of TA systems have been distinguished and classified based on the nature of the antitoxin and the mechanism by which it inactivates its cognate toxin (*Lieven et al. 2005; Markovski and Wickner, 2013; Yarmolinsky, 1995).* In Type I TA systems, the antitoxin is an RNA that interacts with the toxins mRNA to inhibit the synthesis of the toxin's protein (*Gerdes and Wagner, 2007; Fozo et al., 2010*). In Type II TA systems, both toxin and antitoxin are proteins, inhibition of protein toxin is accomplished via physical protein-protein interaction between toxin and antitoxin (*Gerdes et al., 2005*) In type III TA systems, the antitoxin is a small RNA that directly interacts with the protein toxin to inhibit its toxicity (*Blower et al., 2009*). Type IV TA systems toxin and antitoxin don't interact directly, the antitoxin rather functions by stabilizing the target of its toxin instead of directly inhibiting the toxin (*Masuda et al., 2012*). A Type V TA systems antitoxin is a protein that specifically cleaves its toxin's mRNA preventing the translation of the toxin (*Wang et al., 2012*). And unlike the other five types of TA systems, in a Type VI TA system the antitoxin acts as a proteolytic adaptor where it binds its toxin and induces its degradation via cellular proteases (*Akare et al*., 2013). Generally, toxins are stable proteins that hamper an essential process within the cell while antitoxins are labile; as a result, antitoxins must be constantly expressed in order to compensate for their degradation and successfully inhibit their cognate toxins, hence TA systems are referred to as addiction modules (*Yarmolinsky, 1995*).

The most extensively studied TA systems are Type II, mainly due to their abundance on the genomes of many bacterial species and relative ease of identification. Type I and Type III TA systems were difficult to identify as they contain small RNAs (sRNAs). But recent bioinformatic searches based on general characteristics of type I TA systems led to the identification of many type I loci across a large number of bacterial genomes (*Fozo et al., 2010*).

Also, the delay of the discovery of Type IV and V TA systems lead Type II to be the most appropriate TA systems for genetic and functional studies. Functions of TA systems are being extensively investigated as more evidence is linking TA systems to biofilm formation (*Ren et al., 2004; Kim et al., 2009*), persister cell formation (*Maisonneuve et al., 2011; 2013; Amato et al., 2013; Germain et al., 2013*), and general stress response (*Wang et al., 2011; Hu et al., 2012*). Amongst type II TA systems, MazEF and RelBE are the most characterized of all, following is an overview of both:

MazEF:

As a toxin, MazF is a stable protein and specifically cleaves RNAs at ACA sequences (*Zhang et al., 2005*). On the other hand, MazE is labile due to rapid degradation via ClpAP protease and functions to inhibit the RNase activity of MazF by directly binding to it (*Aizenman et al., 1996; Kamada et al., 2003*). Both MazE and MazF naturally exist as dimers and one MazE dimer binds to two MazF dimers forming a hetero-hexamer complex $MazF_2$-$MazE_2$-$MazF_2$ and in this form MazF toxicity is blocked (*Kamada et al., 2003*). MazE-MazF is transcribed as one operon and the two open reading frames are overlapping. This operon is regulated by a negative feed back loop as free MazE as well as $MazF_2$-$MazE_2$-$MazF_2$ complex bind to its promoter and therefore inhibit transcription (*Marianovsky et al., 2001*). Activation of MazF was reported to induce bacteriostatic state which is reported to reach a point of no return after 8 hours and to induce programmed cell death even when MazE was expressed to rescue the culture (*Amitai et al., 2004*).

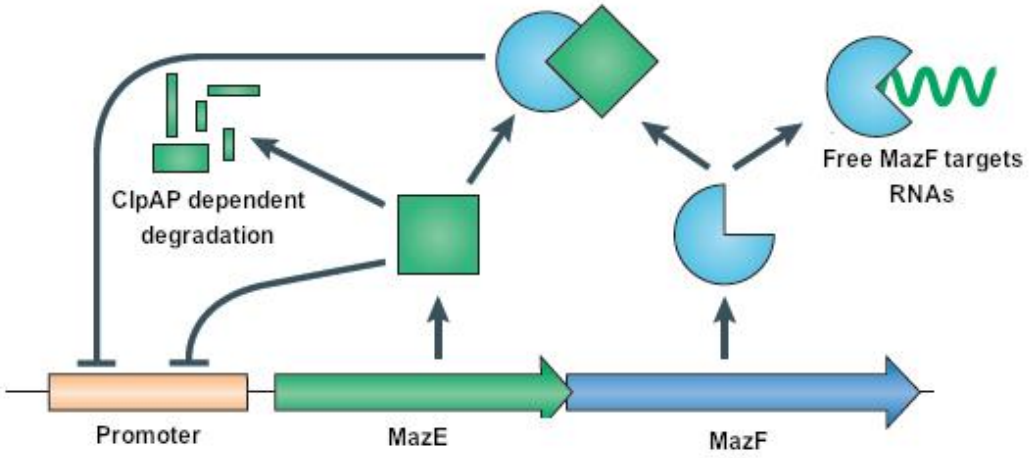

Schematic representation of MazE-MazF Toxin-Antitoxin system regulation

RelBE:

RelBE is also one of the most well studied type II TA systems. Like MazF, the toxin RelE is a ribonuclease but unlike MazF, RelE did not show sequence specificity, rather being translation dependent (*Neubauer et al., 2009*). 3D structure showed that one RelB dimer binds two RelE monomers and blocks their access to the ribosomal A site and induces structural rearrangements that disrupts the endoribonuclease pocket of RelE (*Boggild et al., 2012, Li et al., 2009*). As a type II TA system, RelE is a stable protein while RelB is rapidly degraded via the activity of Lon protease (*Greds et al., 2005*). The transcription of *relBE* is autoregulated, where RelB is a transcription repressor and RelE is a co-repressor (*Gotfredsen et al., 1998*).

Remarks

As I mentioned above, bacteria and phage are in constant struggle in a battle for survival; where bacteria is always trying to acquire new weapons to fight off phages and phages evolve ways to render such weapons useless. Since their discovery, TA systems were linked to many functions in cell physiology generally as stress response systems. Although it was suggested that TA systems might function as antiphage agents, little or no evidence was provided until recently our group reported a type II TA system, RnlAB, and showed that it can counter T4 phage infection in the absence of *dmd* gene of T4. MazEF and RelBE are the most studied type II TA systems and their functions have been established in many stress conditions but they have never been thoroughly investigated their ability to counter phages. In my study I aim to evaluate the ability of MazEF and RelBE to counter T4 phage infections and characterize their interactions with phage components.

Materials and methods

Bacterial strains and Phages

E. coli K-12 strain TY0807 (*sup^0 araD139 hsdR* Δ*lacX74 rpsL araD*$^+$) was used as the wild type (Koga *et al*., 2011). E.coli mutants (TY0807 Δ*MazE-MazF*::*cat, ΔChpBK*-ChpBI::cat and Δ*ChpB*Δ*MazEF::cat* double mutant) was constructed as described (Datsenko and Wanner, 2000). Briefly, a fragment containing a chloramphenicol-resistance cassette flanked by the sequences upstream of *MazE or ChpBK* and downstream of *MazF or ChpBI* was amplified by polymerase chain reaction (PCR) with pKD3 as the template and the primers 5'-AGCGAGCAGGATGTCTGGGGTAAATCCACCCCTGCGGGTGACGAAATATG 5'-TTTTTATGCCCGCGATAAATAAACACACCTTATTCCACCACCGCCTGCAACATATGAATATCCTCCTTAG 5'-GTGTAGGCTGGAGCTGCTTC5′-AGATTGATATATACTGTATCTACATATGATAGCGGTTTGAGGAAAGGGTTTATAGGAACTTCGGCGCGCC and 5′-GGGTCTGTCAGGTGGAAACCTGTGACCAGAATAGAAGTGAGTTAGTAACACGCCTTACGCCCCGCCCTGC. The fragment was introduced into TY0807 harboring pKD46, which encodes λ phage Red, and chloramphenicol-resistant colonies were screened by PCR with primers 5′-ACCTGTGACCAGAATAGAAG and 5′-GGAATTCCATATGATAGCGGTTTGAGG to select Δ*MazE-MazF*::*cat* cells. *E. coli* strains BL21(DE3) or MH1 (Otsuka and Yonesaki, 2005) were used for protein purification or burst size assay.

Bacteriophages were T4D, T2L, and T7 (Simons *et al*., 1987). The Δ*alt* mutant of T4 phage was constructed by the insertion/substitution method (Selick *et al*., 1988) using pBSPL0+Δ*alt* (see below). The *del11* mutant phage has a deletion of multiple genes containing *ModA* and *ModB* located between gene *39* and *56* (Homyk and Weil, 1974).

Construction of plasmids

To construct pBAD24-Flag-*mazF*, a DNA fragment was amplified by PCR using *E. coli* W3110 DNA as the template and the primers 5′-CGGTACCTGATTACAAGGAT GACGACGATAAGATGGTAAGCCGATACGTACC and 5′-CCCGTCGACGTTAGTAACACTACCCAATC (underlined text represents the DNA sequence encoding a FLAG tag). The DNA fragment was digested with *Kpn*I and *Sal*I, and ligated into the corresponding sites of pBAD24 (Guzman *et al*., 1995). pBAD24-Flag-*mazF* was digested with *Bam*HI and *Hin*dIII, and ligated into pBAD33 to construct pBAD33-Flag-*mazF*. To construct pBAD33-Flag-ChpBK a DNA fragment was amplified using W3110 DNA as template and the primers 5′-AGGAATTCACCATGGATTACAAGGATGACGACGATAAGGTAAAGAAAAG TGAATTTGAACGGGG and 5’- GC AAGCTT TTATTCCACCACCGCCTGCAAGCGTAATAACGCC. The generated fragments were digested with *EcoRI* and *HindIII* then ligated to pBAD33. To construct pQE80L- ChpBI a DNA fragment was amplified using W3110 DNA as template and the primers 5′- AC GGATCC CGTATTA CCATAAAAAG ATGGGGGAAC and 5’- AC CTGCAG TTACCATATTTCGTCACCCGCAGGGGTGG. The generated fragments were digested with *BamHI* and *PstI* then ligated to pQE80L. To generate pQE80L-*mazE*, a DNA fragment was amplified using W3110 DNA as template and the primers 5′-GGCATGCATCCACAGTAGCGTAAAGCG and 5′-GGAAGCTTGCTTACCATTACCAGACTTC. The DNA fragment was digested with *Sph*I and *Hin*dIII and ligated into pQE80L. To construct pET21a-*mazEF*-His, the DNA fragment containing *MazE-MazF* was amplified by PCR using W3110 DNA as the template and the primers 5′-GGGGTCTAGAGAGGAAAGGGTTATGATCC and 5′-CTCTCTCGAGCCCAATCAGTACGTTAATTTTGGC, then digested with *Xba*I and *Xho*I, and ligated into pET-21a(+) (Novagen). To construct pQE80L-*alt*, the DNA fragment was PCR-amplified using T4 DNA as the template and primers 5′- GGGGATCCGAACTTATTACAGAATTATTTGACG and 5′-GGGCTGCAGTTATCCTTGAACGAACTTGTAAGGC, digested with *Bam*HI

and *Pst*I, and then ligated into pQE80L. To generate pBSPL0+Δ*alt*, two PCR-amplified fragments were ligated into pBSPL0+ (Selick *et al*., 1988), one by one. First, a DNA fragment was amplified by PCR using T4 DNA as the template and the primers 5′-AGGAATTCGGCCCGAAGGCCTTTAATAATCTATTGG and 5′-AGGTCGACGTGGATTTATTCTTGAGTCAGAGTGTGG, and digested with *Eco*RI and *Sal*I, and then ligated into pBSPL0+. Second, the DNA fragment amplified by PCR using T4 DNA and the primers 5′-AGGGATCCGACACCAATTGGATTTCCACCC and 5′-AGGAATTCCTTATTACAGAATTATTTGACGGCGC was digested with *Eco*RI and *Bam*HI, and ligated into the corresponding sites of the plasmid constructed in the first step.

The MazF mutant plasmids were constructed using a KOD-Plus-Mutagenesis kit (Toyobo) with pBAD33-Flag-*mazF* as the template. Primers used for mutagenesis were: for MazF(R4A), 5′-GCATACGTACCCGATATGGGCGATCTG and 5′-GCTTACCATCTTATCGTCGTCATCC; for MazF(R29A), 5′-GCTCCAGCTGTTGTCC TGAGTCCTTTC and 5′-ATGTCCAGCTTGCTCGCTACC; for MazF(R69A), 5′-GCTGATGGCGTAGCGTTAGCTGATCAGG and 5′-TTCCTGACCGGATAAAACAACTTCG; for MazF(R84A), 5′-GCGGCAAGAGGAGCAACGAAGAAAGGAACAG and 5′-CCAGGCGATACTTTTTACCTGATC; for MazF(R86A), 5′-GCAGGAGCAACGAAGAAAGGAACAGTTG and 5′-TGCCCGCCAGGCGATACTTTTTACCTG; for MazF(R4K), 5′-AAATACGTACCCGATATGGGCGATCTG and 5′-GCTTACCATCTTATCGTCGTCATCC.

Western blot analysis

Proteins were separated by electrophoresis through a 15 or 20% polyacrylamide gel containing SDS and electroblotted onto Immuno-Blot PVDF membrane (Bio-Rad). The membranes were probed with a mouse anti-

FLAG M2 monoclonal antibody (Sigma-Aldrich) or a mouse anti-His antibody (GE Healthcare for N-terminal His-tag and Waco for C-terminal His-tag) and then with horseradish peroxidase-conjugated sheep anti-mouse IgG (GE Healthcare) as a secondary antibody. Proteins were detected with Immobilon Western Chemiluminescent Substrate (Millipore) and an LAS image analyzer (Fujifilm).

Mass spectrometry analysis of modified MazF after T4 infection

TY0807 cells expressing FLAG-MazF were infected with wild-type T4 to induce MazF modification. FLAG-tagged proteins were immunoprecipitated from cell extracts with anti-FLAG M2 affinity beads (Sigma-Aldrich) and then analyzed directly via FT-ICR mass spectrometry. For the MS and MS/MS analysis combined with nano-scale liquid chromatography, recovered proteins were run on a 20% SDS-PAGE gel and then visualized by Coomassie Brilliant Blue (CBB) staining. FLAG-MazF and modified FLAG-MazF were treated with trypsin in gel, applied to the MS and MS/MS system combined with nano-scale liquid chromatography, and the results were analyzed using the MASCOT database server.

Purification of MazF-His, His-MazE and His-Alt

For purification of His-tagged MazF (MazF-His) (van Rensburg and Hergenrother, 2013), *E. coli* BL21(DE3) cells harboring pET21a-*mazEF*-His were grown in 2 l of Luria–Bertani (LB) medium containing ampicillin (50 μg ml^{-1}) at 37°C until the OD_{600} reached 0.7. After IPTG was added to a final concentration of 1 mM, cells were cultured for a further 4 h, harvested and washed with 60 ml of binding buffer (10 mM Tris-HCl pH 7.9, 500 mM NaCl and 10 mM imidazole). MazF-His was purified under denaturing conditions. The cells were resuspended in 20 ml of binding buffer containing 8 M urea and lysed at a duty of 30% for 30 min using a Tomy sonicator UD-201. After centrifugation at 20,000 × *g* for 30 min at 4°C, the clarified lysate was mixed with 1 ml of Ni-NTA Superflow resin (Qiagen) by end-over-end rotation for 30 min at room temperature. The mixture was applied to a gravimetric flow

column, and washed with 100 ml of binding buffer containing 8 M urea to fully dissociate MazE from His-MazF. On-column refolding of His-MazF was achieved by seven washes with 10 ml of binding buffer containing 7 to 0 M of urea, decreasing the urea concentration by 1 M each wash. Washes with binding buffer containing more than 4 M urea were performed at room temperature, and washes containing less than 4 M urea and all subsequent steps were performed at 4°C. After washing with 20 ml of washing buffer (10 mM Tris-HCl pH 7.9, 500 mM NaCl and 60 mM imidazole), MazF-His was eluted with 5 ml of binding buffer containing 250 mM imidazole. To remove non-specific proteins with high intrinsic affinity to Ni-NTA resin, the eluted fraction was diluted with 5 ml of binding buffer and applied to 4 ml of chitin resin (NEB) packed into a column, followed by washing with 8 ml of binding buffer. Flow-through and wash fractions were combined and applied to an Amicon Ultra-15 3 kDa molecular weight cutoff spin concentrator (Millipore) at 4°C to exchange with MazF storage buffer (20 mM sodium phosphate pH 6.0, 0.01% Tween-20, and 50% glycerol) and to concentrate the MazF-His.

For His-tagged MazE (His-MazE) or His-tagged Alt (His-Alt), TY0901 cells harboring pQE80L-*mazE* or TY0807 cells harboring pQE80L-*alt* were grown in 500 ml of LB medium containing ampicillin (50 μg ml^{-1}) at 37°C until the OD_{600} reached 0.6, and IPTG was added to a final concentration of 1 mM. After incubation for 4 h, cells were harvested, resuspended in 8 ml of lysis buffer (50 mM Tris-HCl pH 7.5, 150 mM NaCl, 0.2 mM PMSF, 10 mM Imidazole) containing lysozyme (100 μg ml^{-1}), and incubated on ice for 30 min. Cells were disrupted at a duty of 30% for 5 min using a Tomy sonicator UD-201. The lysate was centrifuged at 10,000 × *g* for 20 min, and the supernatant was loaded onto a column containing 1.5 ml of Ni-NTA Superflow resin (Qiagen) at 4°C. After washing with 40 ml of washing buffer (50 mM Tris-HCl pH 7.5, 150 mM NaCl, 20 mM Imidazole), His-tagged proteins were eluted with 10 ml of elution buffer (50 mM Tris-HCl pH 7.5, 150 mM NaCl, 1 mM DTT, 400 mM Imidazole), dialyzed against buffer (50 mM Tris-HCl pH 7.5, 10 mM NaCl), and concentrated using Amicon Ultra-15 3 kDa devices. In the case of His-MazE, proteins were loaded onto a DEAE-Cellulose (DE52, Whatman) column to remove contaminating proteins. His-MazE was eluted as a single protein at 0.3-0.5 M NaCl, dialyzed against buffer (50 mM Tris-HCl

pH 7.5, 10 mM NaCl) and concentrated using an Amicon Ultra-15 3 kDa concentrator.

In vitro *ADP-ribosylation of MazF by Alt*

Purified MazF-His and/or His-Alt were mixed at the molar ratio of 1:3 in 50 µl of transferase buffer (50 mM Tris-acetate pH 7.5, 22 mM NH_4Cl, 1 mM EDTA, 10 mM β-mercaptoethanol, 10% glycerol) in the presence or absence of 0.5 mM β-NAD^+ (MP Biomedicals, LLC) and incubated at 15°C for appropriate times. After SDS-PAGE, proteins were detected by silver staining or western blotting.

In vitro *RNA cleavage by MazF*

MazF-His and/or His-MazE, or ADP-ribosylated MazF-His were mixed with 1 or 7 pmol of fluorescent labeled RNA [5′-GCUGAACAAAUCAAAUAAUU-FAM-3’] (GeneDesign) in a 70 µl of MazF reaction buffer (20 mM sodium phosphate pH 7.5, 0.05% Tween-20). After incubation at 37°C, 10 µl of samples were withdrawn at the designated times and the RNA was separated through a 20% polyacrylamide gel containing 7 M urea and detected with an FLA-7000 image analyzer (Fujifilm). The signal intensity was quantified using the Image J program.

UV mutagenesis assay

T4Δ*alt* was irradiated with UV light for 11, 14, 18, and 29 seconds followed by appropriate dilutions and plated on TY0901 then incubated at 37°C overnight. Single plaques were then picked by sterile toothpick and stabbed on soft agar containing TY0807 (WT) or TY0901 (Δ*mazEF*).

Labeling of newly synthesized proteins

Cells were grown to a density of 5 x 10^8 cells ml^{-1} at 37°C in M9 minimal medium supplemented with 0.3% casaminoacids, 1 mg ml^{-1} thiamine, 20 mg ml^{-1} tryptophan, and 1% Glycerol as a carbon source and then infected with T4 phage at a multiplicity of infection of 7. [^{35}S]methionine/cysteine (American Radiolabeled Chemicals, St Louis; > 37 Tbq $mmol^{-1}$) was added at 3.7 MBq ml^{-1} to 0.1 ml cultures at various times after infection. After incubation for 3 min, incorporation of radioactive amino acids was terminated by adding 2 µl of 20% of casamino acids and chilling the tubes quickly on ice. Cells were collected by centrifugation and suspended with sample loading buffer. After boiling, labeled proteins were separated with electrophoresis through a 12.5% polyacrylamide containing SDS and analysed with a BAS-1800 image analyser (Fujifilm).

An ADP-ribosyltransferase Alt of bacteriophage T4 negatively regulates the *Escherichia coli* MazF toxin of a toxin–antitoxin module

Abstract

Prokaryotic toxin–antitoxin (TA) systems are linked to many roles in cell physiology, such as plasmid maintenance, stress response, persistence against antibiotics and protection from phage infection, and the activities of toxins are tightly regulated. Here, I describe a novel regulatory mechanism for a toxin of *Escherichia coli* TA systems. The MazF toxin of MazE-MazF, which is one of the most characterized type II TA systems, was modified immediately after infection with bacteriophage T4. Mass spectrometry demonstrated that the molecular weight of this modification was 542 Da, corresponding to a mono-ADP-ribosylation. This modification disappeared in cells infected with T4 phage lacking Alt, which is one of three ADP-ribosyltransferases encoded by T4 phage and is injected together with phage DNA upon infection. *In vivo* and *in vitro* analyses confirmed that T4 Alt ADP-ribosylated MazF at an arginine residue at position 4. Ribonuclease activity assays showed that ADP-ribosylation of MazF by Alt resulted in the reduction of MazF RNA cleavage activity *in vitro*, suggesting that it may function to inactivate MazF during T4 infection. Indeed, T4Δ*alt* phage produced significantly less progeny per infected cell than wild type T4 phage, however this difference was only observable when *E. coli* cells were infected at early log phase but not during later stages. To understand why, I followed the expression of MazE and MazF from early log phase through stationary phase. Interestingly, MazE and MazF were highly expressed in early growth stages

and gradually decreased to unobservable levels under my experimental conditions in later growth stages. This is the first example of the chemical modification of an *E. coli* toxin in TA systems to regulate activity and this is the first clue suggesting that MazEF expression is growth stage dependent.

Introduction

Toxin–antitoxin (TA) systems have been found on plasmids and chromosomes of many bacteria and archaea (*Gerdes et al., 2005*), and genes encoding a cognate toxin and an antitoxin are generally contiguous. Toxins are stable proteins that hamper essential cellular processes, such as DNA replication, translation or cell division (*Jiang et al., 2002; Yamaguchi and Inouye, 2009; Mutschler et al., 2011; Tan et al., 2011; Winther and Gerdes, 2011; Zhang and Inouye, 2011*). Antitoxins are labile (*Buts et al., 2005; Schuster and Bertram, 2013*). As a result, antitoxins must be constantly expressed to compensate for their degradation in order to successfully inhibit their cognate toxins; hence TA systems are referred to as addiction modules (*Yarmolinsky, 1995*). TA systems are mainly divided into two types: antitoxins of type I TA systems are small non-coding RNAs that block the translation of toxin mRNAs (*Gerdes and Wagner, 2007; Fozo et al., 2010*), and in type II TA systems antitoxins are proteins that neutralize the effect of toxins by direct interaction (*Gerdes et al., 2005*). There are actually six different types of TA system, but only a few examples have been discovered in each of types III, IV, V, and VI (*Blower et al., 2009; Masuda et al., 2012; Wang et al., 2012; Akare et al*., 2013).

Functions of TA systems are being extensively investigated as more evidence links TA systems to biofilm formation (*Ren et al., 2004; Kim et al., 2009*), persister cell formation against antibiotics (*Maisonneuve et al., 2011; 2013; Amato et al., 2013; Germain et al., 2013*), general stress response (*Wang et al., 2011; Hu et al., 2012*), and phage defense (*Pecota and Wood, 1996, Fineran et al., 2009, Dy et al., 2014*). Recently, our group reported that two type II TA systems, *rnlA-rnlB*, encoded by the *Escherichia coli* K-12 chromosome (*Koga et al., 2011*), and *lsoA-lsoB* of enterohemorrhagic *E. coli* O157:H7, encoded by a plasmid pOSAK1, (*Otsuka et al., 2012*), play roles as anti-phage mechanisms. Their toxins (*RnlA and LsoA*) with endoribonuclease activities are activated after bacteriophage T4 infection, because T4 infection shuts off *E. coli* gene expression (*Kutter et al., 1994*), resulting in the disappearance of the unstable antitoxins RnlB and LsoB. When a T4 *dmd* mutant infects, free RnlA or LsoA degrade most T4 mRNAs at a late stage of

infection, leading to a defect in T4 propagation (*Kai et al., 1996; Otsuka and Yonesaki, 2005; Koga et al., 2011; Otsuka et al., 2012*). Thus, these TA systems function as phage defense agents. However, when Dmd is expressed immediately after T4 infection, as found in wild-type infection, the phage can grow normally. T4 Dmd, rather than RnlB or LsoB antitoxin, suppresses the RNA cleavage activity of RnlA or LsoA by direct binding (*Koga et al., 2011; Otsuka et al., 2012*). Therefore, T4 phage has evolutionally obtained its own antitoxin against bacterial toxins functioning as an anti-phage mechanism. Sorek's group also showed a similar relationship between T7 phage and bacterial TA systems (*Sberro et al., 2013*): the *sanaTA* system in Shewanella sp. provides resistance against T7 phage lacking the 4.5 gene. These are significant examples demonstrating the arms race between bacteria and phages. *E. coli* K-12 is predicted to possess at least 37 TA systems and, like RnlA and LsoA, most of the type II toxins have endoribonuclease activities (*Yamaguchi and Inouye, 2011; Wang et al., 2012*). Considering that T4 infection immediately shuts off *E. coli* gene expression, I suspect that other type II TA systems might function as anti-phage mechanisms and that T4 phages might encode antitoxins against *E. coli* toxins for their own survival.

In this study, I addressed the relationship between a T4 infection and two of the most characterized type II TA systems, RelB-RelE and MazE-MazF. RelB and MazE are unstable antitoxins because they are constantly degraded by cellular proteases Lon and ClpAP respectively (*Greds et al., 2005; Aizenman et al., 1996*), while both stable RelE and MazF possess RNA cleavage activities where RelE is translation dependent RNase and MazF is translation independent and specifically cleaves RNAs at ACA sequences to block protein synthesis (*Greds et al., 2005; Zhang et al., 2005*). Structural analyses demonstrated that a RelB dimer binds to two RelE monomers to block RelE activity (*Boggild et al., 2012, Li et al., 2009*). On the other hand, both MazE and MazF naturally exist as dimers and a MazE dimer forms a stable complex with two MazF dimers to inhibit MazF toxicity (*Kamada et al., 2003*). A previous report showed that the presence of MazE-MazF resulted in the reduction of P1 phage propagation (*Hazan and Engelberg-Kulka, 2004*), but its function in P1-infected cells remains unclear.

Here, I demonstrate that the growth of T4 phage was significantly increased by the disruption of *MazE-MazF*. This suggests that MazF can function as a phage defense, and also that T4 phage might have an antitoxin against MazF to enable efficient growth. Intriguingly, MazF was ADP-ribosylated by T4 Alt protein immediately after infection, and this modification resulted in the reduction of MazF RNA cleavage activity. I have further validated that MazE-MazF does indeed act as an antiphage mechanism in the absence of T4 Alt ADP-ribosyltransferase. Moreover, my work discovers that MazE-MazF expression is growth stage dependent and is expressed at significantly higher levels during an early-log phase compared to a mid and late-log phase. These findings are very significant in the field of TA systems, and will provide a whole new point of view in addressing the mechanisms underlying the persistence and virulence of bacteria. This is the first example of a chemical modification of a toxin to regulate its activity.

Results

Effect of MazF and RelE on E. coli and T4 phage protein synthesis

The mechanism by which Type II toxins are activated depends on the difference of stability between the toxin and cognate antitoxin. Generally, when cells are exposed to stressful conditions labile antitoxins will be degraded due to the activity of cellular proteases while stable toxins will be freed and activated (*Jiang et al., 2002; Yamaguchi and Inouye, 2009; Mutschler et al., 2011; Tan et al., 2011; Winther and Gerdes, 2011; Zhang and Inouye, 2011*). To replicate the activation of toxins and investigate the effect of toxins on cell or phage Flag tagged *mazF* and *relE* were cloned into the plasmid pBAD33 resulting in the two plasmids pBAD33-F-mazF and pBAD33-F-relE. Then activity of MazF and RelE was addressed via induction from plasmids. TY0807 (used here as wild type) harboring pBAD33-F-mazF, pBAD33-F-relE or empty vector were grown in LB at 37°C until OD_{600} reached 0.5, one culture set was induced with 0.1% L-arabinose while the other was left without induction. As shown in (Fig. 1) induction of MazF and RelE showed severe toxicity inhibiting cell growth, while non-induced cells grew normally. MazF and RelE have an endoribonuclease activity that targets global mRNAs and as a result inhibiting protein synthesis (*Zhang et al., 2005*), in order to investigate whether their inhibitory effect on cell growth is associated with the inhibition effect on protein synthesis, cells harboring pBAD33-F-mazF or pBAD33-F-relE were grown at 37°C in M9C-Glycerol, and newly synthesized proteins were pulse-labeled with [S^{35}] methionine/cysteine before and after induction of MazF and RelE by addition of 0.1% L-arabinose according to the method described in materials and methods (Fig. 2). Before induction of toxins, proteins were prominently labeled, indicating that protein synthesis was active. After induction, incorporation of radioactivity into protein was rapidly reduced and it almost ceased even at 10 min after induction, suggesting that protein synthesis was severely inhibited by actions of MazF and RelE. Now that MazF and RelE toxicity and their effect on cellular protein synthesis were established, I investigated their effect on T4 phage protein

synthesis. Cells harboring pBAD33-F-mazF, pBAD33-F-relE or empty vector were treated 0.1% L-Ara for 30 min then infected with T4 phage at m.o.i of 5, newly synthesized proteins were labeled at different time points using [S^{35}] methionine/cysteine. As shown in (Fig. 3) T4 protein synthesis in cells expressing MazF or RelE was greatly reduced compared to cells with empty vector, interestingly however, weak expression of T4 phage proteins occurred even in the presence of MazF and RelE suggesting that T4 might express inhibitory factors against MazF and RelE of *E. coli*.

Modification of MazF after T4 infection

T4 infection results in the immediate blockage of *E. coli* gene expression (*Kutter et al., 1994*), which may trigger the disappearance of unstable antitoxins (MazE and RelB) and consequently lead to the activation of stable toxins (MazF and RelE). Hence I followed the fate of MazE-MazF and RelB-RelE with or without T4 infection (Fig. 4). For this experiment, I constructed four plasmids, pQE80L-mazE and pQE80L-relB, expressing His-tagged MazE (His-MazE) or His-tagged RelB (His-RelB) under the control of an IPTG-inducible promoter, and pBAD24-Flag-mazF and pBAD24-Flag-relE expressing FLAG-tagged MazF (FLAG-MazF) or FLAG-tagged RelE (FLAG-RelE) under the control of an arabinose-inducible promoter. Cells harboring pQE80L-mazE, pBAD24-Flag-mazF pQE80L-relB or pBAD24-Flag-relE were grown until mid-log phase and then treated with IPTG or L-arabinose to induce respective proteins. After induction, a translational inhibitor, tetracycline or T4 phage, was added to the culture and total proteins were extracted at appropriate times, followed by western blotting using antibodies against the His-tag or FLAG-tag. After the addition of tetracycline, His-RelB was unstable with a half-life of 12 min consistent with previous findings (*Christensen et al., 2001*). After T4 infection RelB was also degraded with a half-life of about 10 min (Fig. 4A). RelE on the other hand was stable both after tetracycline addition and after T4 infection (Fig. 4B). For MazEF TA system, His-MazE was labile with a half-life of 10 min after tetracycline addition (Fig. 4C) and FLAG-MazF was stable (Fig. 4D), which is consistent with previous reports (*Aizenman et al., 1996; Sat et al., 2001*). After T4

infection, His-MazE disappeared with a half-life of 3.5 min (Fig. 4C). Further destabilization of MazE and RelB after T4 infection compared with MazE and RelB levels without infection suggests the activation of protease(s) to degrade those antitoxins, but I presently have no idea about a mechanism or a factor for the rapid degradation of MazE and RelB after infection. Interestingly, after T4 infection, a portion of the FLAG-MazF was converted into a species migrating slightly slower than the native protein (Fig. 4D), suggesting a chemical modification of MazF. To further shed light on this post-translational modification of MazF I thought it will be useful to investigate whether this modification is specific only to T4 phage infection or not. Cells expressing FLAG-MazF were infected with T4 related phage T2 and T4 unrelated phage T7, the modification of MazF appeared only in cells infected with T4 phage, but not in cells infected with T2 or T7 phages (Fig. 5). In an effort to understand this chemical modification, unmodified and modified FLAG-MazF were immunoprecipitated from T4-infected cells by anti-FLAG M2 affinity beads and applied to FT-ICR mass spectrometry. Figure 6 shows that the difference in molecular weight between unmodified and modified FLAG-MazF was 542 Da, which is a mass corresponding to the addition of an ADP-ribosyl group.

ADP-ribosylation of MazF after T4 infection

Because a chemical modification of a toxin of a bacterial TA system was never observed before, I decided to focus on investigating MazF modification further. MazF modification occurred immediately after T4 infection (Fig. 4D). This strongly suggested that the factor responsible for MazF modification was expressed immediately after infection or injected together with phage DNA upon infection. Considering that a molecular weight difference of 542 Da corresponds to the addition of one ADP-ribosyl group, the modification of MazF after T4 infection is likely to be a mono-ADP-ribosylation through the activity of an ADP-ribosyltransferase expressed by T4. An ADP-ribosyltransferase catalyzes the transfer of an ADP-ribosyl group from the substrate, nicotinamide adenine dinucleotide (β-NAD^+), to a specific amino

acid on the acceptor protein, frequently arginine or histidine (the reaction is illustrated in Fig. 7). T4 phage is known to ADP-ribosylate many *E. coli* proteins shortly after infection through the activity of three enzymes, ModA, ModB, and Alt (*Rohrer et al., 1975; Depping et al., 2005*), the activity of which facilitate gaining control over the infected host cell primarily through shifting gene expression towards T4 genes at different stages of phage growth (*Corda and Di Girolamo, 2003*). ModA and ModB are synthesized shortly after T4 infection and mainly ADP-ribosylate the α-subunit of host RNA polymerase and the S1 ribosomal protein, while Alt is injected together with phage DNA upon infection and many host proteins are targets for Alt, including the host RNA polymerase. To investigate whether any of these enzymes is responsible for MazF modification, cells expressing FLAG-MazF were either treated with tetracycline to stop translation or infected with wild-type, Δ*del11* (a deletion mutant of modA and modB), or Δ*alt* T4 phage. Cell extracts were separated by sodium dodecyl sulfate polyacrylamide gel electrophoresis (SDS-PAGE) and examined by western blotting (Fig. 8A). MazF modification occurred in cells infected with wild-type T4 or Δ*del11*, but not in cells infected with T4 Δ*alt*, strongly suggesting that MazF modification after infection is catalyzed by T4 Alt. To further confirm this, cells were co-transformed with pBAD33-Flag-*mazF* and pQE80L-*alt* and the modification of MazF examined in the presence or absence of Alt without T4 infection. Expression of His-Alt together with FLAG-MazF resulted in the appearance of modified FLAG-MazF (Fig. 8B).

Alt transfers one ADP-ribose moiety from β-NAD+ to an arginine residue on the acceptor protein (*Rohrer et al., 1975*) and MazF contains five arginines (Fig. 8C). To identify which arginine is modified, I first compared trypsin-digests of unmodified and modified MazF using a MS and MS/MS system combined with nano-scale liquid chromatography and the MASCOT database server (Table 1). Due to limitations of this method, I was able to detect protein fragments spanning 78% and 73% of both MazF and modified MazF respectively; comparing the molecular masses of detected fragments showed no differences in mass and spanned three arginines (R29, R69, and R84) out of the five in MazF, this result leads me to believe that one of the non-covered arginines is the site of ADP-ribosylation. Next, I used plasmids expressing

FLAG-MazF mutants in each of which one of the five arginine residues was substituted with alanine. After T4 infection, FLAG-MazF mutants were analyzed by SDS-PAGE and western blotting (Fig. 9A). I detected a slower migrating species than the original form of the cognate protein for variants R29A, R69A, R84A and R86A, indicating that these arginines are not the target of modification. Only FLAG-MazF R4A did not generate a slower migrating species after T4 infection, though its migration rate was somewhat different from the other mutants and the wild type protein. To further confirm that Arg4 is the target of modification, I used a plasmid expressing a FLAG-MazF mutant R4K, in which the arginine at position 4 was substituted with lysine, and found that it migrated at a similar rate to wild type MazF as a single species before and after T4 infection (Fig. 9B).

In vitro ADP-ribosylation of MazF

To further confirm ADP-ribosylation of MazF by T4 Alt, I performed *in vitro* ADP-ribosylation assays using purified MazF-His and His-Alt. Since a previous report demonstrated that the ADP-ribosyltransferase activity of Alt decreased to 20% after incubation for 15 min at 37°C (*Rohrer et al., 1975*), assays were carried out at 15°C. MazF was modified in the presence of Alt and β-NAD+ as an ADP-ribose donor, but the modification did not occur in the absence of either Alt or β-NAD+ (Fig. 10). As seen in Figure 10, modified MazF never exceeded 50% of the total MazF under my experimental conditions. Also, the modification of MazF seemed to plateau at 50% *in vivo* (Fig. 4D). To confirm this assumption, I tested the modification of MazF while gradually increasing the amount of His-Alt *in vitro* (Fig. 11) and found that indeed the modification plateaus at 50%. Also, as MazE is usually bound to MazF under normal growth conditions, it is important to evaluate the effect of MazE on MazF ADP-ribosylation by Alt. To investigate this idea, purified MazF and Alt were mixed in the presence or absence of MazE or/and NAD^+. As shown in Figure 12, MazE did not interfere with MazF modification *in vitro* by Alt and MazF was ADP-ribosylated both in the presence and absence of MazE at a similar rate. Taken together, I conclude that MazF is ADP-

ribosylated by T4 Alt at Arg4 and only 50% of MazF is ADP-ribosylated by Alt and this modification is MazE independent.

Reduction of MazF RNA endoribonuclease activity by ADP-ribosylation

MazF specifically cleaves RNAs at ACA sequences (*Zhang et al., 2005*). To evaluate MazF activity *in vitro*, I designed a 20 nucleotide RNA containing an ACA sequence after the fifth nucleotide from the 5′-end. Its 3′-end was linked to FAM, a fluorescent probe, to facilitate the detection of the products (Fig. 13A). When MazF-His alone was incubated with the substrate RNA, a band corresponding to the cleavage product of MazF was clearly observed (Fig. 13B, lane 5). As expected, MazF activity was completely abolished when MazE was added to the reaction mixture (Fig. 13B, lane 4).

Generally, ADP-ribosylation of proteins alters their activities. For example, ADP-ribosylation of the α-subunit of *E. coli* RNA polymerase by Alt enhances viral transcription (*Sommer et al., 2000*). In order to investigate the impact of ADP-ribosylation on MazF activity, I first incubated MazF-His and His-Alt in the presence or absence of β-NAD+ (Fig. 13C). Then, a part of reaction mixtures at 3 h after incubation was examined for the endoribonuclease activity of MazF. As shown in Fig. 14D, MazF incubated in a reaction mixture without β-NAD+ efficiently cleaved RNA. However, the mixture containing approximately 50% modified MazF exhibited an initial RNA cleavage activity reduced by 69.2% ± 22.9% compared with that of native MazF (Fig. 13E). This result strongly suggests that the ADP-ribosylation of MazF negatively regulates its RNA cleavage activity.

Effect of MazE-MazF on the growth of T4 phage

In order to evaluate the effect of the ADP-ribosylation on MazF activity and consequently on T4 phage growth, it is important to first investigate the effect of MazE-MazF on the growth of T4 phage, for that purpose I measured the

number of progeny phages per T4-infected cell (burst size) (Fig. 14). The burst size in wild-type cells was 71.7 ± 8.3, while it was 100.7 ± 9 in a deletion mutant of MazE-MazF, this increase in phage number produced per infected cell indicates that the MazE-MazF TA system partially, but not completely, suppresses T4 growth, somewhat consistent with the data shown in Fig. 3 for T4 protein synthesis after MazF induction. Since MazE-MazF negatively affected T4 propagation, I suspected that it might function as an anti-phage defense and also that T4 phage might encode an inhibitory factor to block the anti-phage defense mediated by MazE-MazF because T4 phage grow relatively vigorously on cells with endogenous MazE-MazF.

Effect of Alt on T4 phage growth in vivo

ADP-ribosylation of MazF resulted in significant activity loss *in vitro*. In light of this finding, I examined the burst size of wild type T4 and compared it to that of Δ*alt*. Surprisingly, the burst size between of T4 phage and ∆alt T4 phage in wild type *E.coli* was similar (Fig. 15) suggesting that Alt did not contribute in MazF inactivation after T4 infection. However, taking in consideration that 1. *E.coli* lacking *mazEF* produced a burst size significantly higher than that of wild type (Fig. 14) and this burst size increase was resolved up on increasing induction of MazEF from a plasmid (Fig.16), 2. MazE was rapidly degraded after T4 infection, 3. The fact that ADP-ribosylated MazF lost activity *in vitro*; taken together, MazF affects T4 growth and Alt affects MazF activity, thus, Alt must have an effect on T4 growth in the presence of MazF however Alt effect was not observed under my experimental conditions likely due to the presence of an MazEF homologue, ChpBK (toxin)- ChpBI (antitoxin) (*Masuda et al., 1993*). Ideally, if ChpBK activity is not affected by Alt-induced modification, the effect of Alt on T4 growth might not be detectable due to a synergetic effect of MazF and ChpBK. To address this issue, I first followed the stability of ChpBK and ChpBI with and without T4 infection (Fig. 17). Although ChpBI seemed more stable than MazE after tetracycline addition, it was further destabilized after T4 infection. As expected, ChpBK was stable after tetracycline addition, but

unlike MazF no modification appeared on ChpBK after T4 infection, this result suggests that Alt doesn't play a role in ChpBK regulation and ChpBK might be activated after T4 infection, which might mask the effect of Alt on MazF activity.

To address this issue, I measured the burst size of wild type and Δ*alt* T4 in Δ*chpB E. coli.* As I expected, although Alt did not seem to have an effect on ChpBK, the BS of T4 was significantly higher than that of Δ*alt* mutant (Fig. 18). For the first time, I was able to observe significant difference in BS between T4 and Δ*alt* T4 phage likely due to the synergetic effect of MazF and ChpBK. If my assumption is true, then this growth difference should be resolved in cells lacking both *mazEF* and *chpB.* To confirm my finding, I constructed a Δ*mazEF*Δ*chpB* double mutant *E.coli* cells and measured the burst size of wild type and Δ*alt* T4 in wild type, Δ*mazEF, Δchp*B*, and* Δ*mazEF*Δ*chpB E. coli cells.* Again, as I expected, WT T4 produced higher BS than Δ*alt* T4 in Δ*chpB* cells and this difference was resolved in both Δ*mazEF* and Δ*mazEF*Δ*chpB* mutant cells (Fig. 19). Intriguingly however, although WT and Δ*alt* T4 produced similar BS in WT *E.coli* in previous experiment (Fig. 15), WT T4 produced significantly higher BS than Δ*alt* T4 in WT *E.coli* in this experiment and the numbers were comparable to BS numbers in Δ*chpB* mutant (Fig. 19), those results suggest that the BS difference was not due to synergetic effect of MazF and ChpBK but likely to be due to reasons related to experimental conditions. Surely, results in figure 15 and results in figure 19 were obtained under similar conditions the only difference however was that cells were infected with T4 phages at different cell densities; in figure 15 cells were infected at OD_{600} of 0.4 while they were infected at OD_{600} of 0.2 in figure 19. This observation suggests that MazF activity is higher in younger cells than older ones and MazF expression might be growth stage dependent. To follow up with this observation, I used pUC19-p-His-*mazE-mazF*-FLAG plasmid where “p” is the *mazEF* operon native promoter, “His” and “FLAG” are His and FLAG tags respectively. Using this plasmid, I can follow the expression levels of MazE and MazF under the control of their own promoter at different stages of cell growth via western blotting. As shown in (Fig. 20) MazF expression levels were quite high in early-log phase and gradually decreased as cells proceeded to mid-log and stationary phases to almost

unobservable levels. Similarly, MazE was levels decreased significantly as cell density increased. To my knowledge, this is the first time MazEF expression is shown to be stage dependent and this observation clearly explains the BS difference between WT T4 and Δ*alt* T4 phages.

MazEF does act as antiphage agent and T4 might possess multiple mechanisms to inactivate MazF and the ADP-ribosylation of MazF via Alt accounts only for one of these mechanisms. In an effort to uncover other mechanisms that might contribute to MazF inactivation, T4Δ*alt* was UV irradiated to induce random mutations then phages were screened for the ability to grow on Δ*mazEF* cells but not wild type. As shown in table 2, a total of 2772 single plaques were tested. Unfortunately no promising candidates were found. Keeping in mind that *E.coli* encodes for at least 37 TA systems, and many of those systems belong to the MazEF family, it is very likely that other agent(s) that might contribute to MazF inactivation after T4 infection are essential for phage growth and thus cannot be elucidated by this screening method.

Discussion

In this study, I developed a line of evidence indicating that a factor of T4 phage, Alt, adds a mono-ADP-ribose onto MazF toxin, which leads to a significant loss of MazF activity. When T4 phage infected *E. coli* cells expressing exogenous MazF, approximately 50% of the exogenous MazF was modified (Fig. 4D). Mass spectrometry analysis (Fig. 6) indicated that the molecular weight of this modification was 542 Da. Since this size corresponded to a mono ADP-ribosylation and T4 phage is known to ADP-ribosylate many *E. coli* proteins immediately after infection for its own efficient growth, I suspected that MazF is ADP-ribosylated after T4 infection. My *in vivo* (Fig. 8A and B) and *in vitro* (Fig. 10) analyses confirmed that the modification of MazF is ADP-ribosylation and that the ADP-ribosyltransferase encoded by T4 phage, Alt, is required for this modification. Also, I demonstrated the reduction of MazF RNA cleavage activity by the ADP-ribosylation *in vitro* (Fig. 13D and E). Moreover, T4 phage lacking *alt* produced significantly less progeny than WT T4 in the presence of MazF, this progeny difference was only observable in young cells during early-log phase but not in later growth stages suggesting that MazF activity might be stage dependent. Surely, western blotting for MazE-MazF levels regulated by their own native promoter showed significantly higher levels of MazE-MazF in early growth stages and this high level expression was gradually reduced as cells multiplied. This is the first report to show that MazEF expression is stage

dependent and the first example of the chemical modification of an *E. coli* toxin in TA systems to regulate activity.

T4 phage encodes three ADP-ribosyltransferases, Alt, ModA and ModB (*Rohrer et al., 1975; Corda and Di Girolamo, 2003; Depping et al., 2005*), and only Alt is responsible for ADP-ribosylation of MazF (Fig. 8A). Alt is packaged into a T4 phage particle and carried into the cell with phage DNA through infection. It was identified as an enzyme to ADP-ribosylate the α-subunit of *E. coli* RNA polymerase and presumably contributes to the preferential transcription from T4 early promoters immediately after infection. Rüger's group detected 27 target *E. coli* proteins ADP-ribosylated *in vitro* by Alt using two-dimensional gel electrophoresis and 10 of them identified by electrospray ionization mass spectrometry analysis were involved in either translation or cellular metabolism (*Depping et al., 2005*), although MazF and the α-subunit of host RNA polymerase were not among the 10 proteins. Because of the delivery of Alt into the cell immediately after infection, ADP-ribosylation of many *E. coli* proteins by Alt is suggested to play roles in the rapid shift of gene expression from *E. coli* to T4, but its biological function is still unknown.

I noticed that the ratio of ADP-ribosylated MazF by Alt *in vivo* (Fig. 4D) and *in vitro* (Fig. 10 and Fig. 11) never exceed 50% even if the amount of Alt or the incubation time was increased, which is similar to a previous result that purified Alt ADP-ribosylated only 50% of the α-subunit of *E. coli* RNA polymerase (*Rohrer et al., 1975*). In fact, Alt adds an ADP-ribosyl group on only one of the two α-subunits of *E. coli* RNA polymerase. Since MazF naturally exists as a dimer (*Kamada et al., 2003*), like α-subunits of RNA polymerase, I believe that Alt modifies only one subunit of the MazF dimer.

Furthermore, the fact that the RNA cleavage activity of MazF significantly reduced when approximately 50% of MazF was ADP-ribosylated (Fig. 13D and E) suggests that Alt should play a role as an inhibitory factor against free MazF in order to enhance the efficient growth of T4. To address this possibility, I compared the burst size between wild-type and Δ*alt* phages in wild-type cells. Against expectations, I could not observe a clear difference between wild-type and Δ*alt* phages. Because MazE was rapidly degraded after T4 infection and ADP-ribosylated MazF activity was significantly reduced compared to native MazF, I suspected that Alt indeed plays a role in MazF regulation but it was not observable under my experimental settings. Further investigation showed that MazF expression was stage dependent and thus the effect of Alt on T4 phage growth was only observable when cells were infected with T4 phage at early-log phase. Even at early stages of cell growth MazF seems to reduce T4 progeny production but not completely shut it down even in the absence of Alt, as MazE is rapidly degraded after T4 infection and thus MazF should be activated I suspect that T4 phage might possess multiple mechanisms to prevent MazF activation after T4 infection. I tried screening for other factors that might be responsible for MazF inactivation after T4 infection using radiation mutagenesis (Table 2) but the search was was unfruitful. Just like Dmd of T4, it is very likely that these factors are essential for phage growth and cant be elucidated through mutagenesis. I also tried to pull-down experiments for MazF after T4 infection but detection of MazF expressed from its own promoter using CBB or Silver staining is very difficult due to the extremely low levels of expression of MazF and

consequently any proteins that might associate with it are extremely difficult to find.

I identified an arginine at position 4 of MazF to be the site of ADP-ribosyl group modification after T4 infection (Fig. 9). Interestingly, toxicity analysis of five MazF arginine mutants showed that the toxicity was completely abolished in an R86A mutant (Fig. 21), Arg86 is a highly conserved amino acid and seems to be essential for MazF activity. Based on the crystal structure of MazF (Fig. 22), Arg4 locates in close proximity to Arg86 (PDB ID: 1UB4, *Kamada et al., 2003*). As shown in figure 22, it is possible that an ADP-ribosyl group on Arg4 might interact with R86 or could block the active site of MazF ribonuclease by steric hindrance, or change the charge around the active site, thereby resulting in the loss of the interaction between MazF and substrate RNAs or of the MazF activity itself.

ADP-ribosylation of MazF occurred after infection with T4 phage, but not with T2 or T7 phages (Fig. 5). My BLAST search indicated that T7 has no homolog of T4 Alt and T2 has a possible homolog with 70% identity (Fig 23). The candidate Alt of T2 phage would not target MazF for ADP-ribosylation. Considering that infection with T2 and T7 phages shuts off host gene expression as for T4 phage, unstable MazE should disappear and consequently MazF should be activated. If so, T2 and T7 phages might have other mechanisms to inactivate free MazF for their own survival.

Our group recently reported a factor other than the cognate antitoxin for directly regulating the activity of a toxin (*Naka et al., 2014*). The RnlA toxin with endoribonuclease activity of an *E. coli* RnlA-RnlB TA system is activated after T4 infection (*Koga et al., 2011*) and this activation requires *E. coli* RNase

HI, which is an endoribonuclease, that cleaves the RNA of a DNA-RNA duplex to remove the RNA primer for DNA replication (*Miller et al., 1973; Itoh and Tomizawa, 1980*). RNase HI enhances the RNA cleavage activity of RnlA *in vitro* and the toxicity of RnlA *in vivo*. This is the only external factor known to directly activate a toxin. However, the mechanism of RnlA activation by RNase HI remains unclear. Taken together with MazF modification by Alt, TA systems might be more complex and versatile than believed to be so far. Also, the fact that MazEF expression is stage dependent is of high importance due to the fact that TA systems are known to affect persistence, virulence, biofilm formation and total cell fitness; therefore it is important to address the effect of TA systems on cell physiology at different stages, understanding such effects will greatly enhance our understanding of disease causing bacteria and developing novel strategies to fight them. Finally, bacteria and phages may have a variety of unknown mechanisms to regulate toxin activities.

Figures

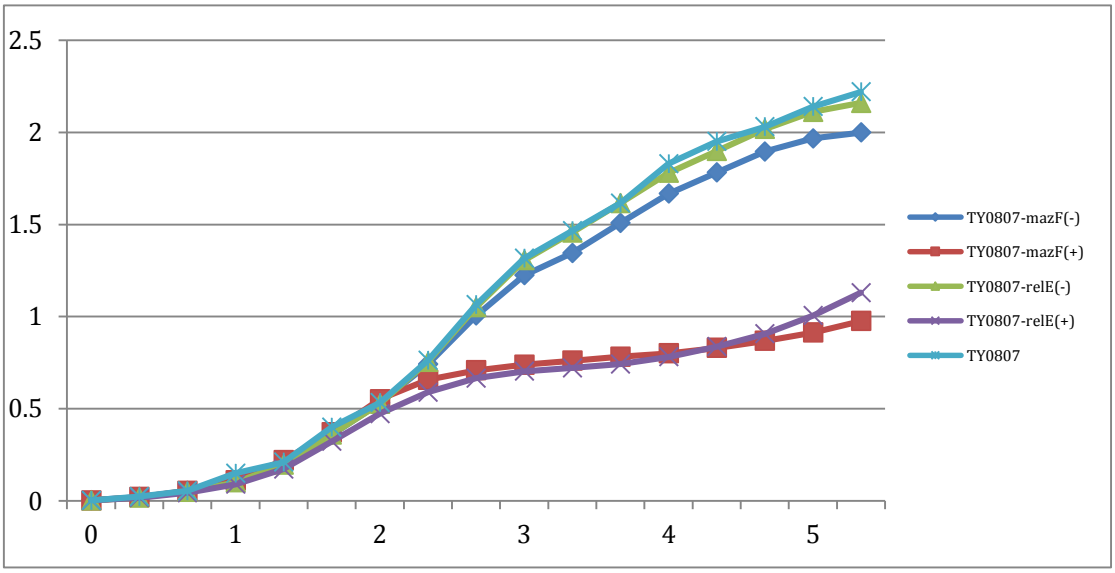

Figure 1. TY0807 harboring pBAD33-F-mazF, pBAD33-F-relE or empty vector were grown in LB at 37°C at OD600= 0.5, one set was induced with 0.1% L-Arabinose while the other set was left without induction, following cell density after induction show the severity of MazF and RelE on cell growth.

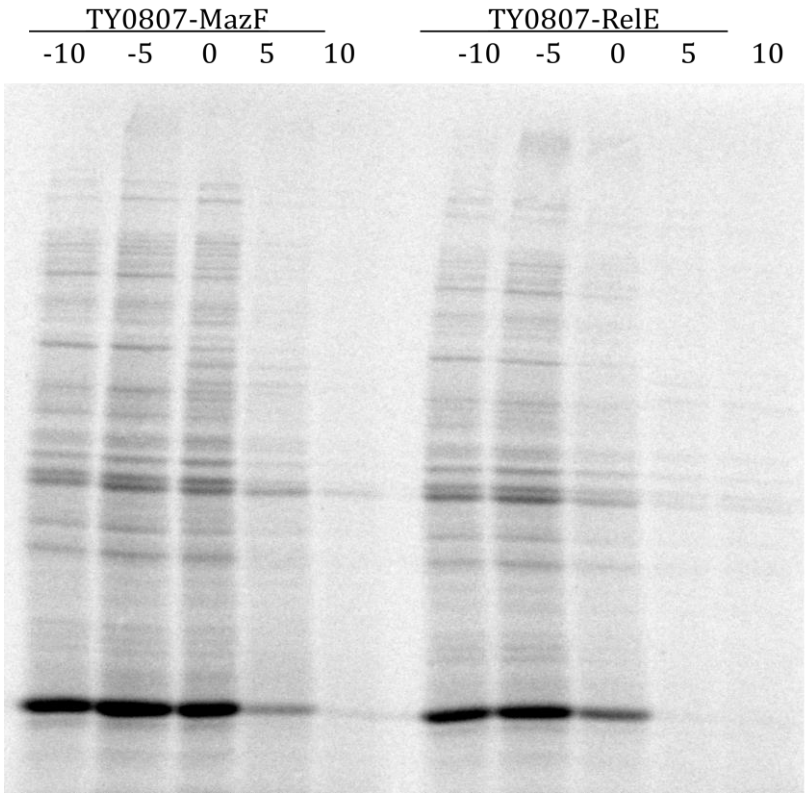

Figure 2. Protein synthesis of TY0807 harboring either pBAD33-F-mazF (left) or pBAD33-F-relE (right) before and after induction with 0.1% L-Arabinose. MazF and RelE are global protein synthesis inhibitors.

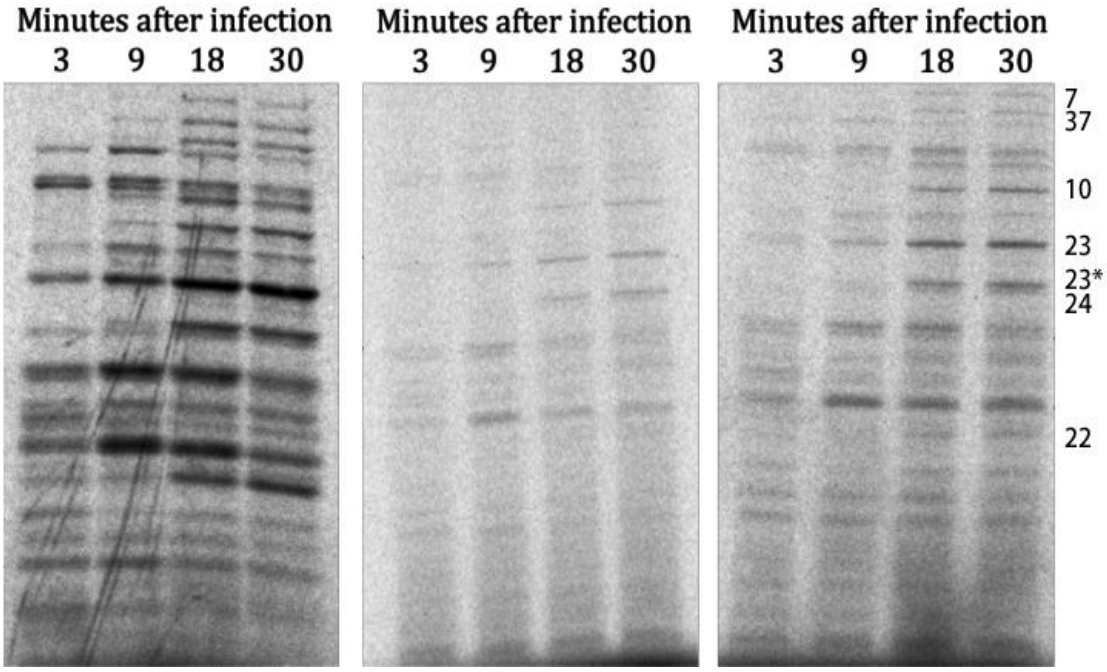

Figure 3. WT *E.coli* cells harboring empty vector (Left), pBAD33-F-relE (Middle) or pBAD24-F-mazF (Right) were treated with L-Ara for 30 min then infected with T4 phage and newly synthesized proteins were followed via pulse labeling as described in materials and methods.

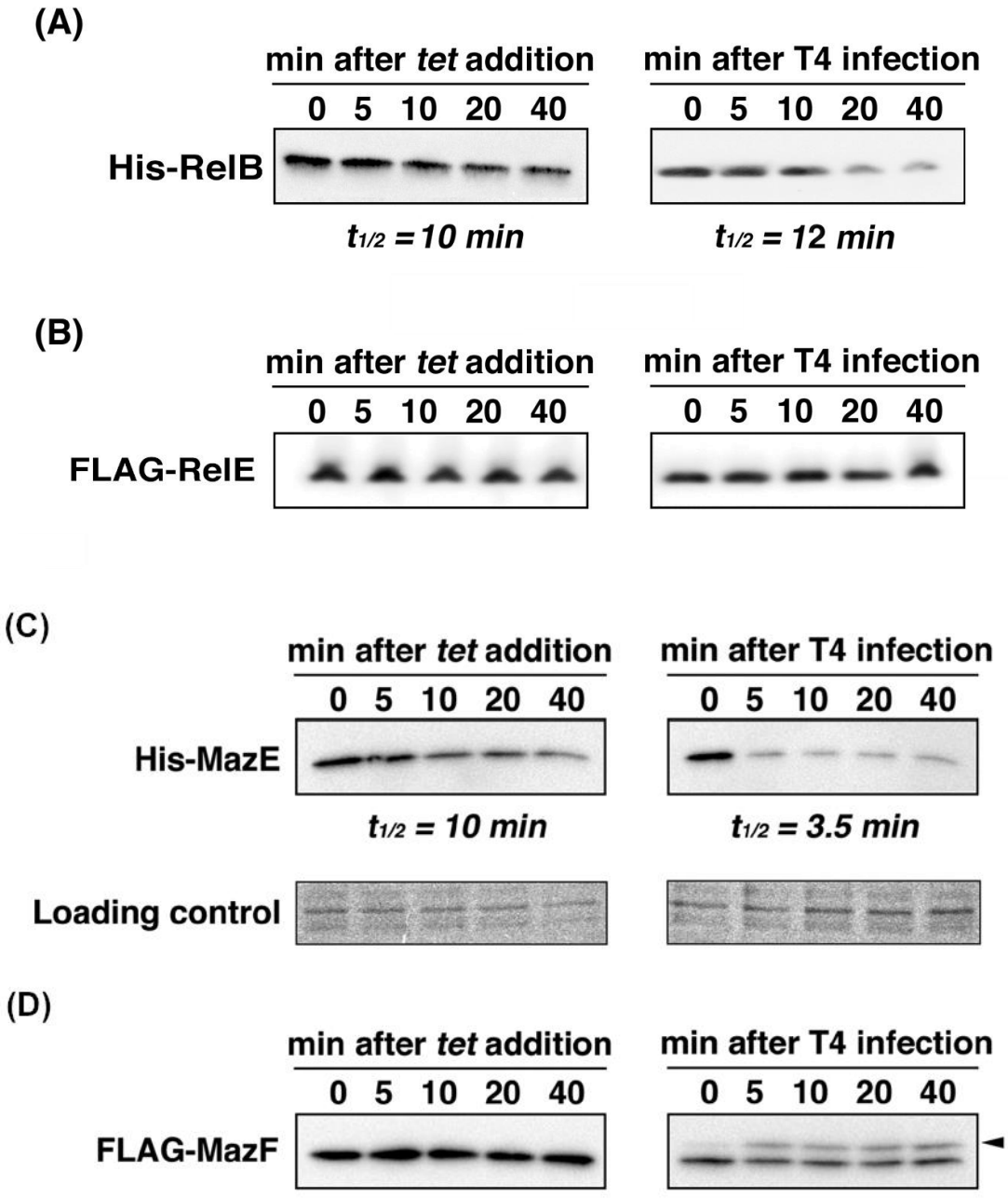

Figure 4. Stabilities of RelB, RelE, MazE and MazF before and after T4 infection.

TY0807 cells harboring pQE80L-*relB* (A) or pQE80L-*mazE* (C) were grown in M9C medium (M9-glucose medium supplemented with 0.3% casamino acids, 1 μg ml^{-1} thiamine and 20 μg ml^{-1} tryptophan) until the OD_{600} reached 0.4. IPTG was added to a final concentration of 0.05 mM and cells were further incubated for 60 min at 37°C, then treated with a translational inhibitor,

tetracycline, at the final concentration of 20 μg ml^{-1}, or infected with T4 phage at a m.o.i. of 5. TY0807 cells harboring pBAD24-Flag-*relE* (B) or pBAD24-Flag-*mazF* (D) were grown in LB medium until the OD_{600} reached 0.4, L-arabinose was added to a final concentration of 0.05% and cells were further incubated for 60 min at 37°C and then treated with tetracycline or infected with T4 phage at a m.o.i. of 5. Total proteins were extracted at the indicated times after the addition of tetracycline or infection with T4, and analyzed by 20% SDS-PAGE, followed by western blotting with antibodies against His-tag or FLAG-tag. The signal intensities of His-MazE and His-RelB were quantified using the Image J program and the time required for a 50% reduction was taken as the half-life ($t_{1/2}$) shown below the figure. The arrowhead indicates the slower migrating species of FLAG-MazF.

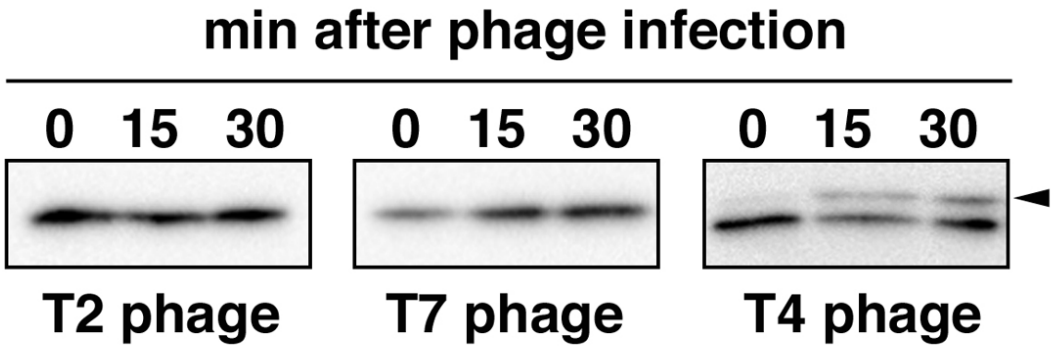

Figure 5. MazF modification is specific to T4 phage.

TY0807 cells harboring pBAD24-Flag-*mazF* were grown to an OD_{600} of 0.4 and FLAG-MazF was induced with L-arabinose at a final concentration of 0.05%, then cells were infected with T4, T2, or T7 phages at a m.o.i. of 5. Total proteins extracted at the indicated times after infection were separated on 20% SDS-PAGE, followed by western blotting with the antibody against FLAG-tag. The arrowhead shows the slower migrating species of FLAG-MazF. ADP-ribosylation of MazF occurs after infection with T4 phage, but not with T2 and T7 phages.

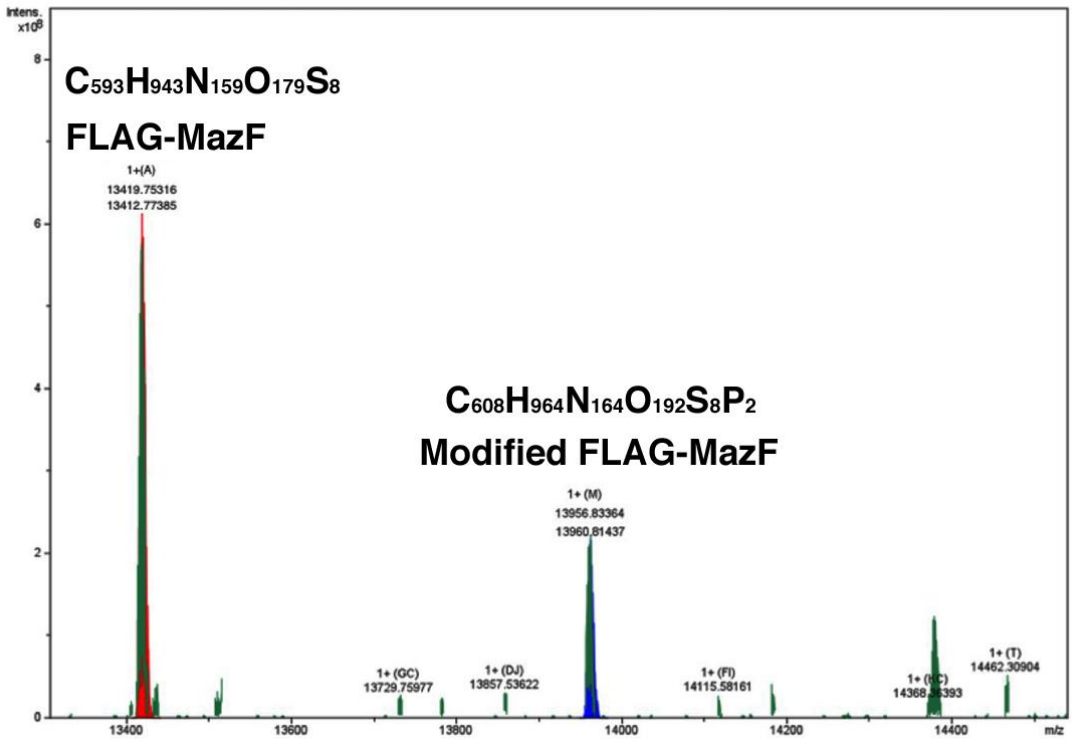

Figure 6. Mass spectrometry analysis of unmodified and modified MazF.

Unmodified and modified FLAG-MazF were immunoprecipitated with an antibody against FLAG-tag and applied to FT-ICR mass spectrometry. Green peaks indicate raw molecular mass data and red or blue peaks represent hypothetical molecular masses of unmodified or modified FLAG-MazF, respectively.

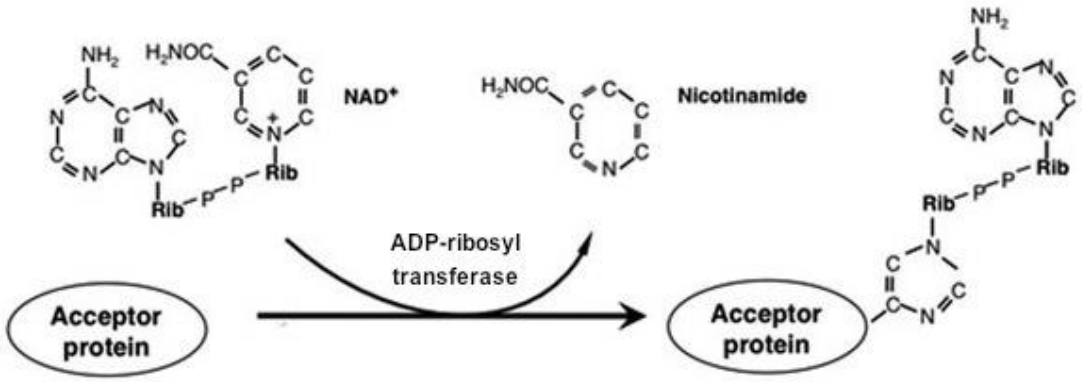

Figure 7. Schematic representation of an ADP-ribosylation reaction

An ADP-ribosyl transferase catalyzes the transfer of an ADP-ribose group from the substrate, nicotinamide adenine dinucleotide (β-NAD+), to a specific amino acid of the acceptor protein.

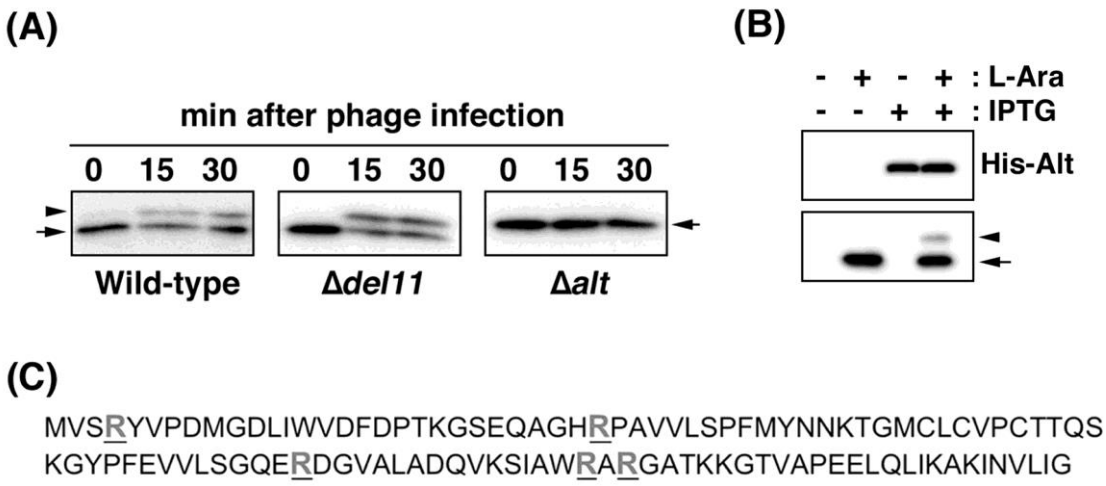

Figure 8. ADP-ribosylation of MazF by T4 Alt.

(A) TY0807 cells expressing FLAG-MazF were infected with T4 wild-type, Δ*del11*, or Δ*alt*, and total proteins extracted at 0, 15 or 30 min after infection were separated on 20% SDS-PAGE, followed by western blotting with the antibody against FLAG-tag. The arrow and arrowhead show the original and the slower migrating species of FLAG-MazF, respectively. (B) TY0807 cells harboring pBAD33-Flag-*mazF* and pQE80L-*alt* were treated with (+) or without (−) 0.1 mM IPTG for 30 min at 37°C when the OD_{600} reached 0.4. Then, cells were treated with (+) or without (−) 0.1% L-arabinose for another 30 min. Total proteins were separated by 15% SDS-PAGE and analyzed by western blotting with the antibody against His-tag (upper panel) or FLAG-tag (lower panel). The arrow and arrowhead show the original and the slower migrating species of FLAG-MazF, respectively. (C) The amino acid sequence of MazF with arginines underlined.

Protein name	Coverage (%)	Start-End	Identified peptide	Theoretical Mr	Calculated Mr
Endoribonuclease MazF (Modified)	73	5–21	R.YVPDMGDLIWVDFDPTK.G	2009.9161	2009.9445
		22-42	K.GSEQAGHRPAVVLSPFMYNNK.T	2301.0983	2301.1324
		57-69	K.GYPFEVVLSGQER.D	1479.7151	1479.7358
		57-69	K.GYPFEVVLSGQER.D	1479.7152	1479.7358
		57-69	K.GYPFEVVLSGQER.D	1479.7181	1479.7358
		57-69	K.GYPFEVVLSGQER.D	1479.72	1479.7358
		57-79	K.GYPFEVVLSGQERDGVALADQVK.S	2476.2256	2476.2598
		57-79	K.GYPFEVVLSGQERDGVALADQVK.S	2476.2294	2476.2598
		70-79	R.DGVALADQVK.S	1014.5224	1014.5346
		91-103	K.KGTVAPEELQLIK.A	1424.8074	1424.8239
		92-103	K.KGTVAPEELQLIK.A	1296.7164	1296.7289
		92-105	K.GTVAPEELQLIKAK.I	1495.8427	1495.861
		104-111	K.AKINVLIG.-	826.52	826.5276
Endoribonuclease MazF (Native)	78	5–21	R.YVPDMGDLIWVDFDPTK.G	2009.9302	2009.9445
		5–21	R.YVPDMGDLIWVDFDPTK.G	2009.9381	2009.9445
		22-42	K.GSEQAGHRPAVVLSPFMYNNK.T	2301.1222	2301.1324
		22-42	K.GSEQAGHRPAVVLSPFMYNNK.T	2301.1415	2301.1324
		57-69	K.GYPFEVVLSGQER.D	1479.7348	1479.7358
		57-69	K.GYPFEVVLSGQER.D	1379.7359	1479.7358
		57-69	K.GYPFEVVLSGQER.D	1479.7368	1479.7358
		57-79	K.GYPFEVVLSGQERDGVALADQVK.S	2476.2232	2476.2598
		57-79	K.GYPFEVVLSGQERDGVALADQVK.S	2476.2393	2476.2598
		57-79	K.GYPFEVVLSGQERDGVALADQVK.S	2476.2511	2476.2598
		57-79	K.GYPFEVVLSGQERDGVALADQVK.S	2476.2529	2476.2598
		70-79	R.DGVALADQVK.S	1014.5303	1014.5346
		70-84	R.DGVALADQVKSIAWR.A	1627.8632	1627.8682
		70-84	R.DGVALADQVKSIAWR.A	1627.8634	1627.8682
		91-103	K.KGTVAPEELQLIK.A	1424.8197	1424.8239
		91-103	K.KGTVAPEELQLIK.A	1424.8234	1424.8239
		92-103	K.GTVAPEELQLIK.A	1296.7286	1296.7289
		92-105	K.GTVAPEELQLIKAK.I	1495.8588	1495.861
		104-111	K.AKINVLIG.-	826.5317	826.5276

Table 1. Mass spectrometry combined with nano-scale liquid chromatography of modified MazF.

TY0807 cells expressing FLAG-MazF were infected with T4 wild-type to induce MazF modification. Total proteins extracted 5 min after infection were applied to an anti-FLAG M2 affinity gel to recover FLAG-tagged proteins. After SDS-PAGE and CBB staining, bands corresponding to FLAG-MazF and modified FLAG-MazF were cut out and used for in-gel trypsinization. Digested protein fragments were identified by MS and MS/MS combined with nano-scale liquid chromatography and analyzed via the MASCOT database server.

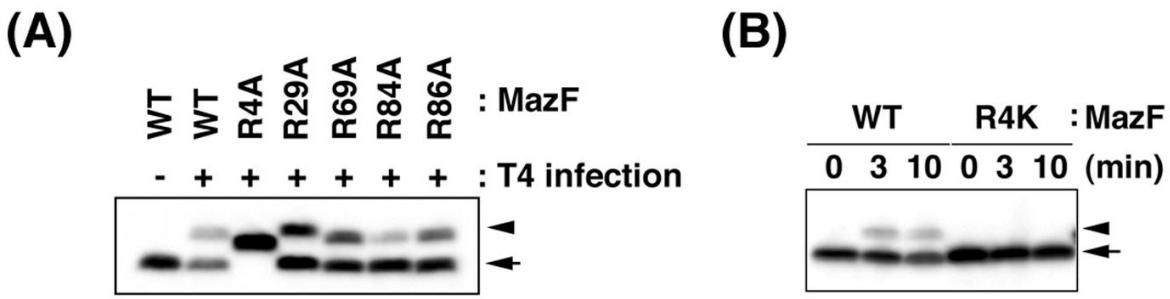

Figure 9. Identification of ADP-ribosylation site on MazF by T4 Alt.

TY0807 cells harboring plasmids expressing wild-type or mutants of MazF were infected with (+) or without (−) T4 wild-type. Total proteins extracted at 10 min (A) or 0, 3, or 10 min (B) after infection were analyzed by 15% SDS-PAGE and western blotting with the antibody against FLAG-tag.

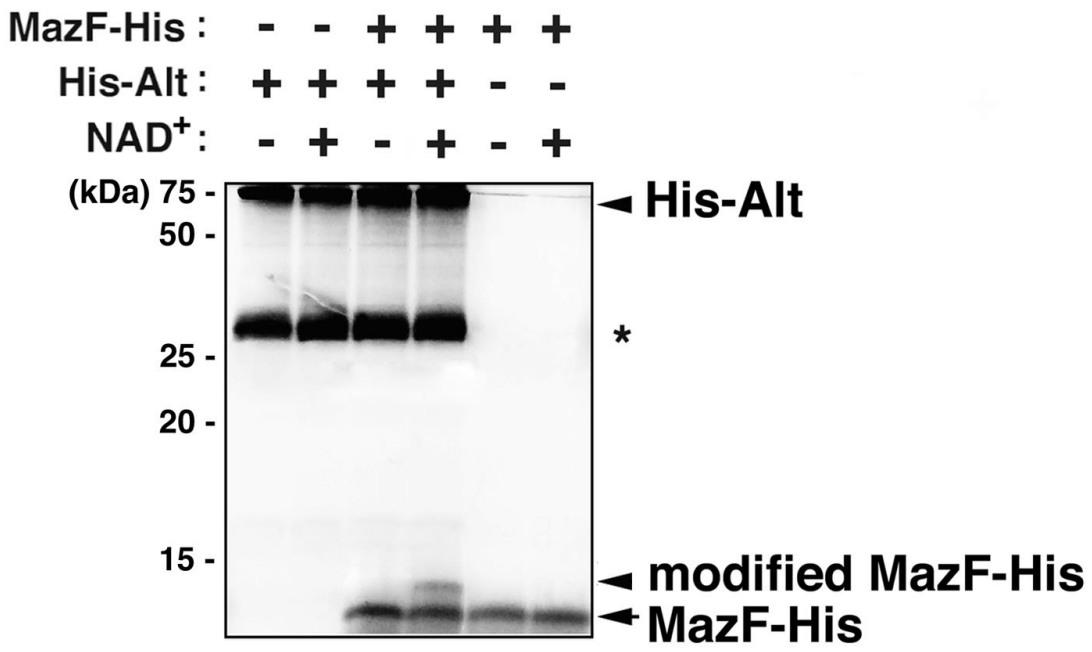

Figure 10. *In vitro* ADP-ribosylation of MazF.

His-tagged Alt (12.5 μg) and/or 0.5 μg of His-tagged MazF were mixed in 50 μl of transferase buffer with (+) or without (−) β-NAD^+ and incubated at 15°C for 3 h. Each reaction mixture (15 μl) was analyzed by 20% SDS-PAGE, followed by silver staining. The asterisk indicates a degradation product of His-Alt.

Figure 11. ADP-ribosylation of MazF *in vitro*.

(A) His-tagged MazF (0.125 μg) and 0, 0.525, 1.05, 3.15, or 5.25 μg of His-tagged Alt were mixed in transferase buffer at a molar ratio of 1:0, 1:0.5, 1:1, 1:3, or 1:5, respectively, in the presence of β-NAD^+ and incubated at 15°C for 3 h. Proteins were separated on 20% SDS-PAGE and analyzed by western blotting with the antibody against His-tag. The asterisk indicates a degradation product of His-Alt. Approximately 50% of MazF was modified even with an excess amount of Alt.

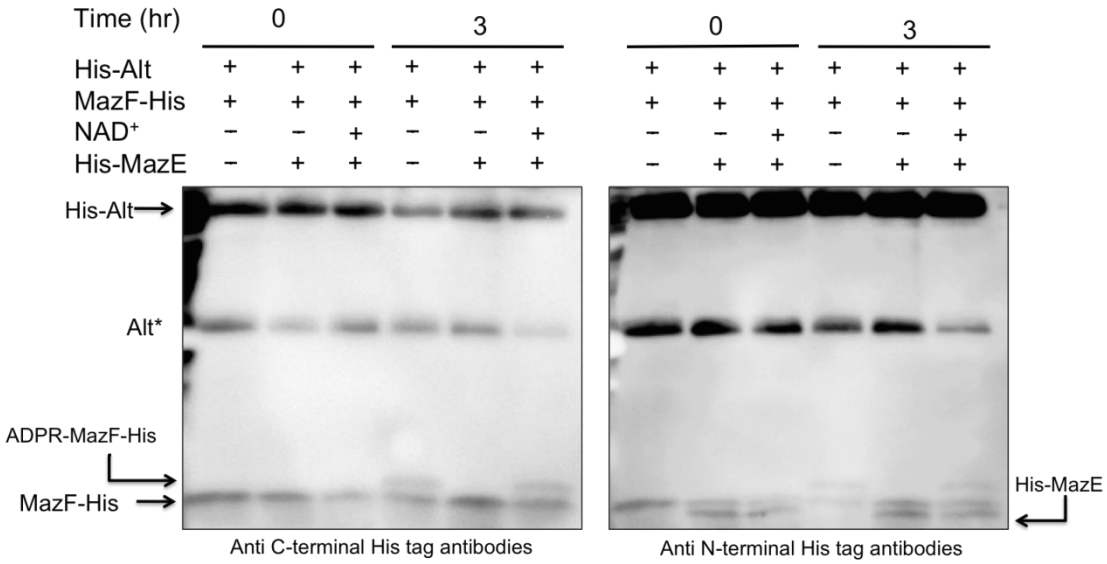

Figure 12. Effect of MazE on MazF ADP-ribosylation by Alt.

His-tagged Alt (12.5 μg) and/or 0.5 μg of His-tagged MazF were mixed in 50 μl of transferase buffer with (+) or without (−) β-NAD^+ or 0.25μg His-MazE and incubated at 15°C for 3 h. Each reaction mixture (15 μl) was analyzed by 20% SDS-PAGE, followed by western blotting. The asterisk indicates a degradation product of His-Alt. Membrane was incubated with primary antibodies against C-terminal His-tag (Wako) (left) then washed and reincubated with primary antibodies against N-terminal His-tag (GE Health) (right).

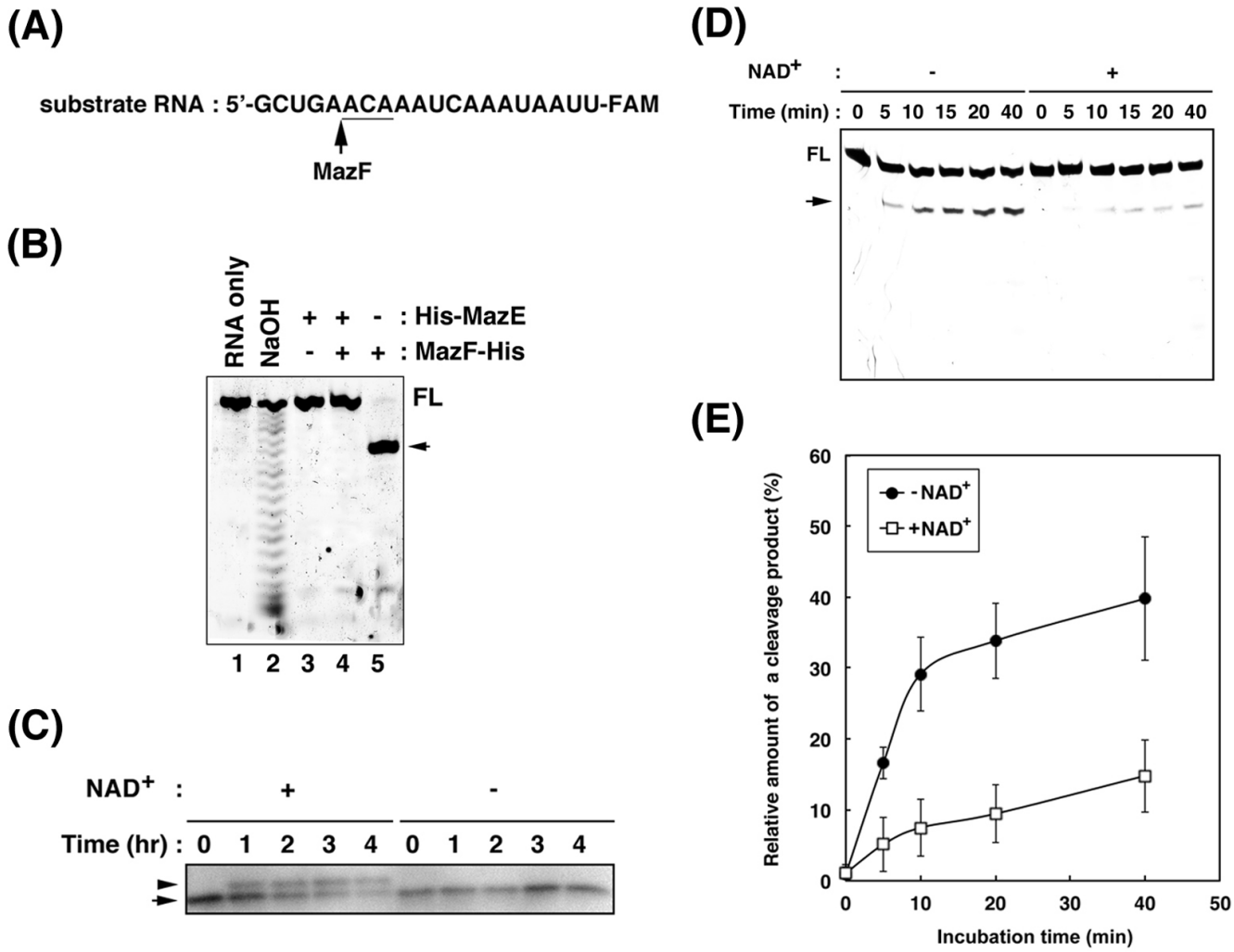

Figure 13. Effect of ADP-ribosylation on MazF endoribonuclease activity.

(A) The sequence of FAM labeled RNA used for MazF RNA cleavage assay is shown. The underline and the arrow indicate the recognition sequence and the cleavage site of MazF, respectively. (B) His-tagged MazF (5 ng) and/or 5 ng of His-tagged MazE were mixed in 10 μl MazF reaction buffer and incubated on ice for 15 min, then 1 pmol of FAM-labeled RNA was added to the reaction mixture and incubated for 15 min at 37°C. The RNA was analyzed by 20% polyacrylamide gel containing 7 M urea. The RNA was partially digested with NaOH (alkaline hydrolysis, lane 2). The arrow indicates the product cleaved by MazF. (C) His-tagged Alt (12.5 μg) and 0.5 μg of His-

tagged MazF were mixed in 50 µl of transferase buffer with (+) or without (−) β-NAD^+ and incubated at 15°C for 0, 1, 2, 3, or 4 h. Each reaction mixture (12.5 µl) was analyzed by 20% SDS-PAGE, followed by western blotting with the antibody against His-tag. The arrow and arrowhead show the original and the slower migrating species of MazF-His, respectively. (D) A part of the reaction mixtures at 3 h after incubation from figure panel (C) were mixed with 7 pmol FAM-labeled RNA in 70 µl of MazF reaction buffer at the final concentration of 0.5 ng μl^{-1} MazF, and incubated at 37°C. Reaction mixture (10 µl) was analyzed at the indicated times by 20% polyacrylamide gel containing 7 M urea. Experiments were performed at least three times and similar results were obtained for each experiment. A representative result is shown. (E) Quantification analysis of MazF RNA cleavage activity was performed. The signal intensities of the MazF cleavage product and full-length RNA were quantified using the Image J program and the relative amount of the cleavage product against input RNA at each time point was plotted. Data points represent the mean and standard deviation of independent triplicate experiments.

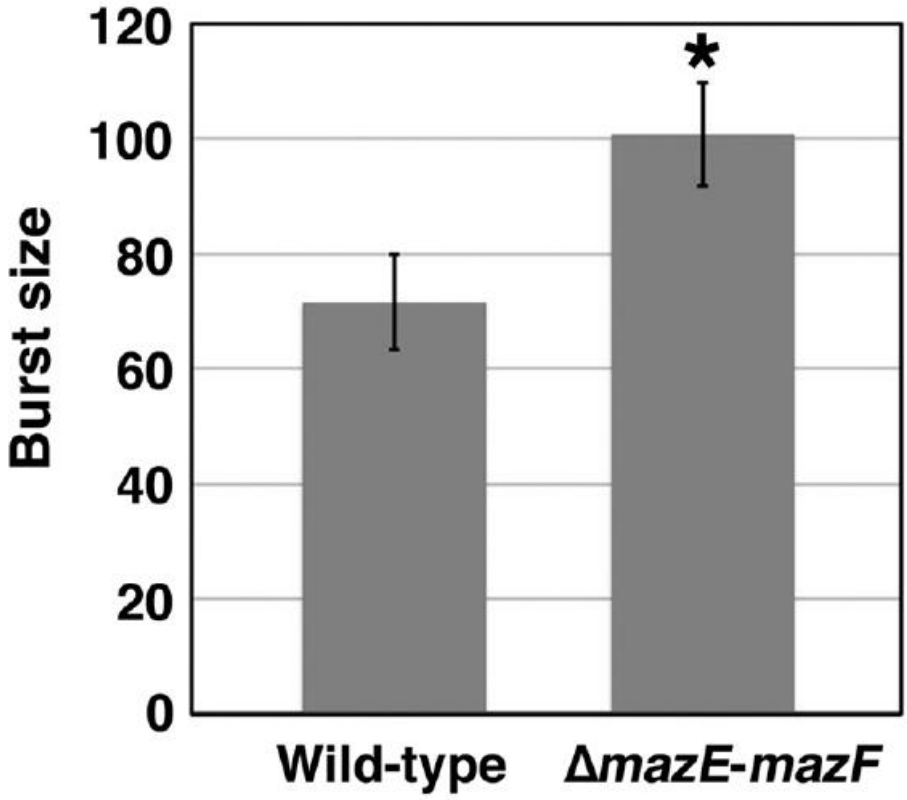

Figure 14. Effect of *MazE-MazF* on the growth of T4 phage.

TY0807 (wild-type) and TY0901 (Δ*MazE-MazF*::*cat*) cells were grown in LB medium until the OD_{600} reached 0.4, and infected with T4 wild-type phage at a multiplicity of infection (m.o.i.) of 0.1 at 37°C. At 8 min, the cells were diluted 10^4-fold with fresh LB medium and further incubated for 70 min. After the cells were lysed with chloroform, the total number of progeny phage particles was determined by plating with MH1 cells as an indicator. The burst size shown in the bar graph is the ratio of the number of progeny to the number of input phage particles. Each value indicates the mean and standard deviation of three independent experiments. *P < 0.05.

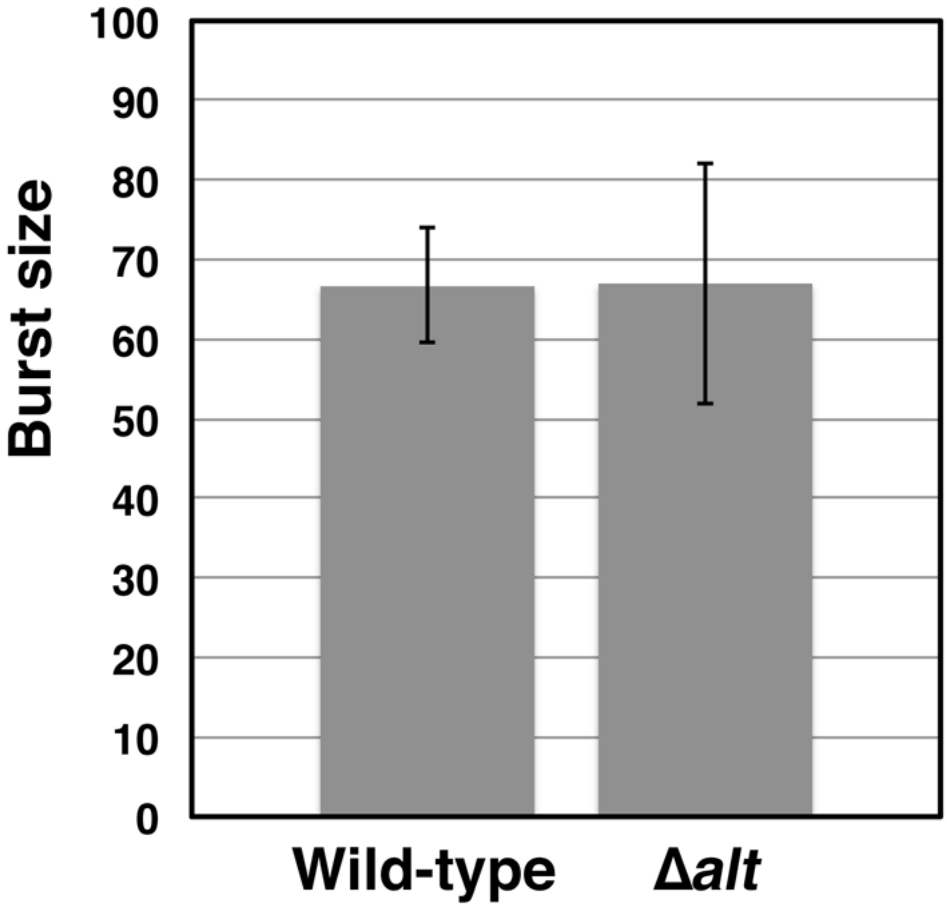

Figure 15. Effect of *alt* on the growth of T4 phage.

TY0807 cells were grown in LB medium until the OD_{600} reached 0.4, and then infected with T4 wild-type or Δ*alt* mutant phage at a m.o.i. of 0.1 at 37°C. At 8 min, the cells were diluted 10^4-fold with fresh LB medium and further incubated for 70 min. After the cells were lysed with chloroform, the total number of progeny phage particles was determined by plating with MH1 cells as an indicator. The burst size is the ratio of the number of progeny to the number of input phage particle and is shown in the bar graph. Each value indicates the mean and standard deviation of three independent experiments. Deletion of *alt* has no effect on T4 growth.

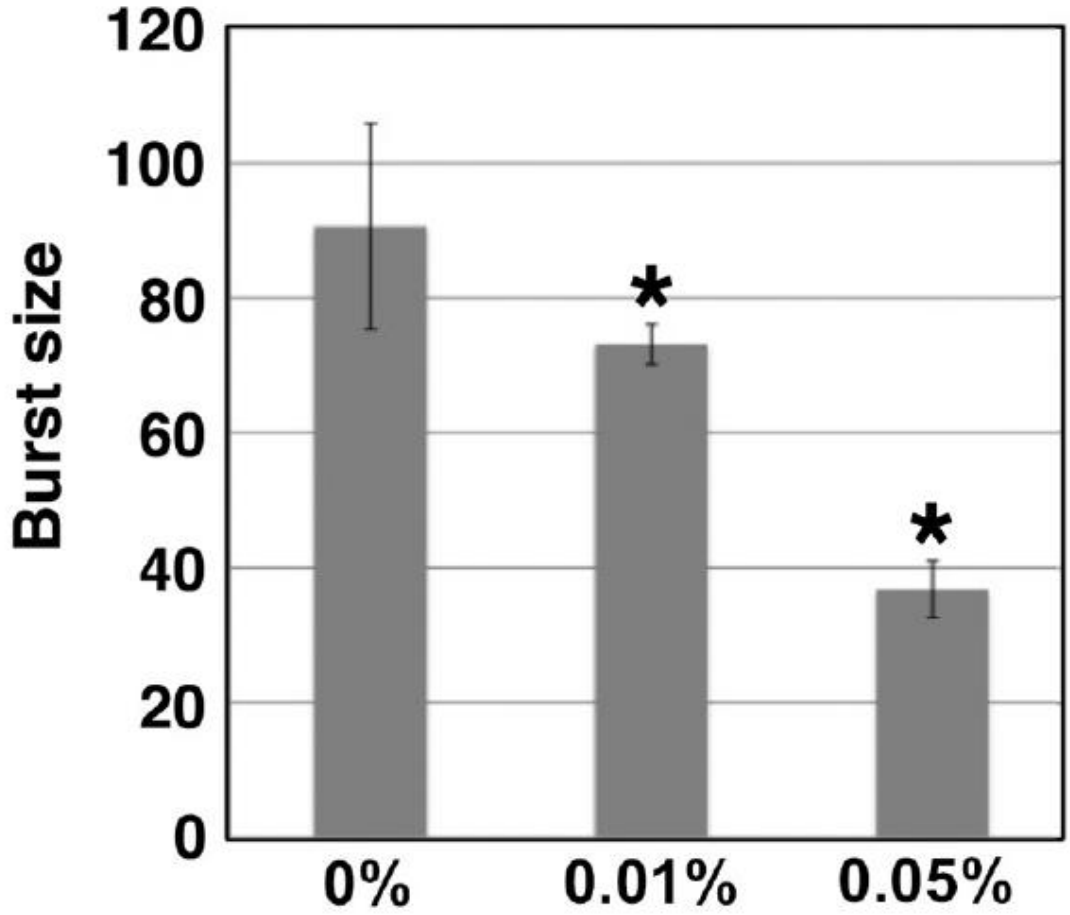

Figure 16. Effect of MazEF on the growth of T4 phage.

TY0901 cells were grown in LB medium containing 0%, 0.01%, or 0.05% L-Arabinose until the OD_{600} reached 0.4, and then infected with T4 wild-type phage at a m.o.i. of 0.1 at 37°C. At 8 min, the cells were diluted 10^4-fold with fresh LB medium and further incubated for 70 min. After the cells were lysed with chloroform, the total number of progeny phage particles was determined by plating with MH1 cells as an indicator. The burst size is the ratio of the number of progeny to the number of input phage particle and is shown in the bar graph. *$P < 0.05$

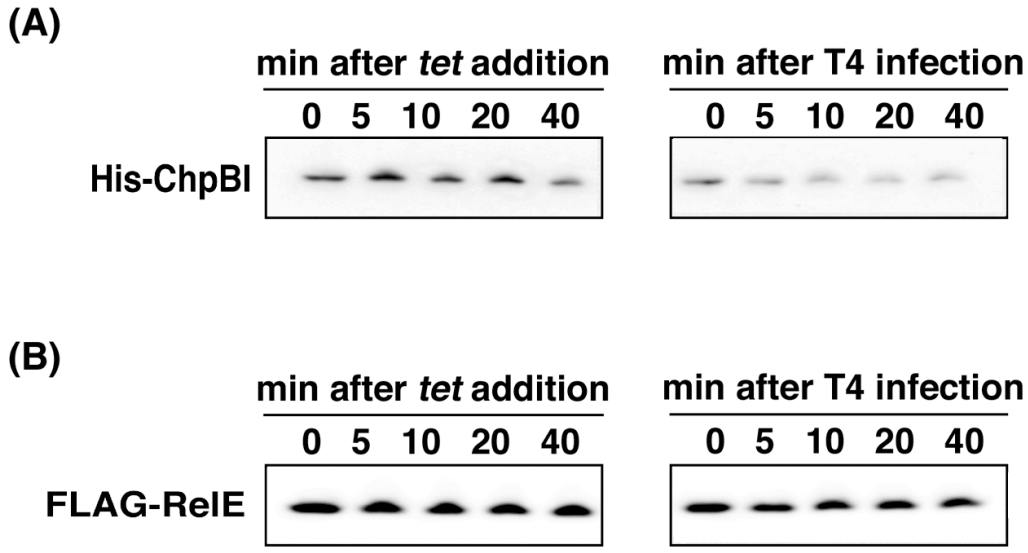

Figure 17. Stabilities of ChpBI and ChpBK before and after T4 infection.

TY0807 cells harboring pQE80L-*chpBI* (A) were grown in LB medium until the OD_{600} reached 0.4. IPTG was added to a final concentration of 0.05 mM and cells were further incubated for 60 min at 37°C, then treated with a translational inhibitor, tetracycline, at the final concentration of 20 μg ml^{-1}, or infected with T4 phage at a m.o.i. of 5. TY0807 cells harboring pBAD24-Flag-*chpBK* (B) were grown in LB medium until the OD_{600} reached 0.4, L-arabinose was added to a final concentration of 0.05% and cells were further incubated for 60 min at 37°C and then treated with tetracycline or infected with T4 phage at a m.o.i. of 5. Total proteins were extracted at the indicated times after the addition of tetracycline or infection with T4, and analyzed by 20% SDS-PAGE, followed by western blotting with antibodies against His-tag or FLAG-tag.

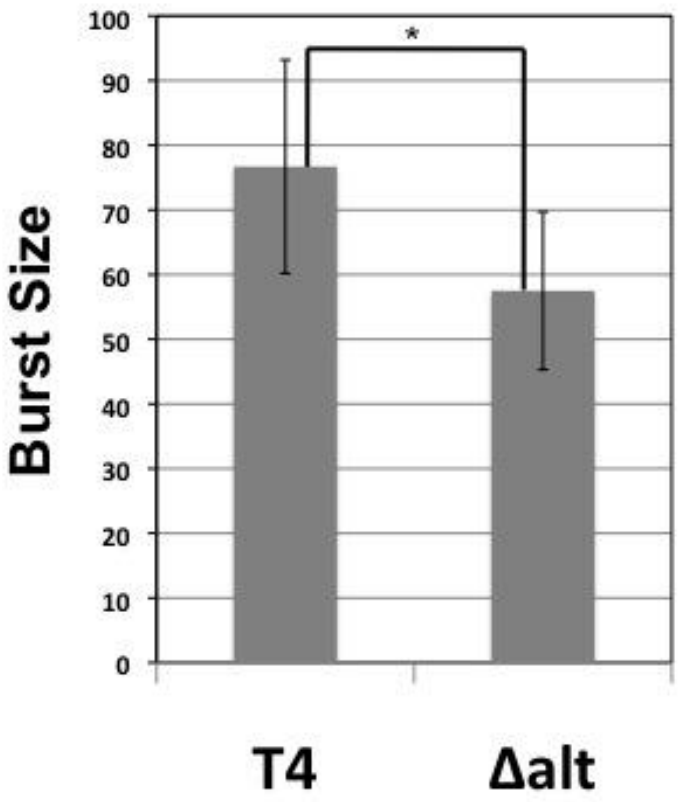

Figure 18. Effect of Alt on the growth of T4 phage.

TY0807 Δ*chpB* cells were grown in LB medium until the OD_{600} reached 0.2, and then infected with T4 wild-type phage at a m.o.i. of 0.1 at 37°C. At 8 min, the cells were diluted 10^4-fold with fresh LB medium and further incubated for 70 min. After the cells were lysed with chloroform, the total number of progeny phage particles was determined by plating with MH1 cells as an indicator. The burst size is the ratio of the number of progeny to the number of input phage particle and is shown in the bar graph. *P < 0.05.

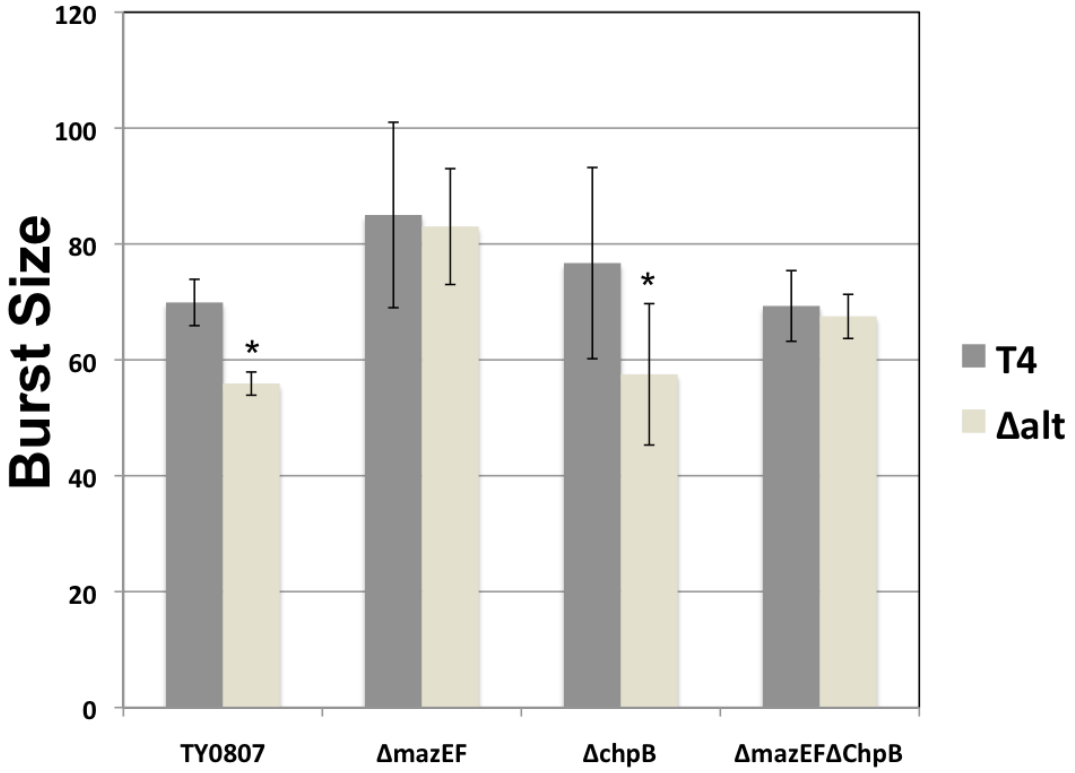

Figure 19. Effect of Alt on the growth of T4 phage.

TY0807, Δ*mazEF*, Δ*chpB* or Δ*mazEF*Δ*chpB* cells were grown in LB medium until the OD_{600} reached 0.2, and then infected with T4 wild-type phage at a m.o.i. of 0.1 at 37°C. At 8 min, the cells were diluted 10^4-fold with fresh LB medium and further incubated for 70 min. After the cells were lysed with chloroform, the total number of progeny phage particles was determined by plating with MH1 cells as an indicator. The burst size is the ratio of the number of progeny to the number of input phage particle and is shown in the bar graph. *P < 0.05.

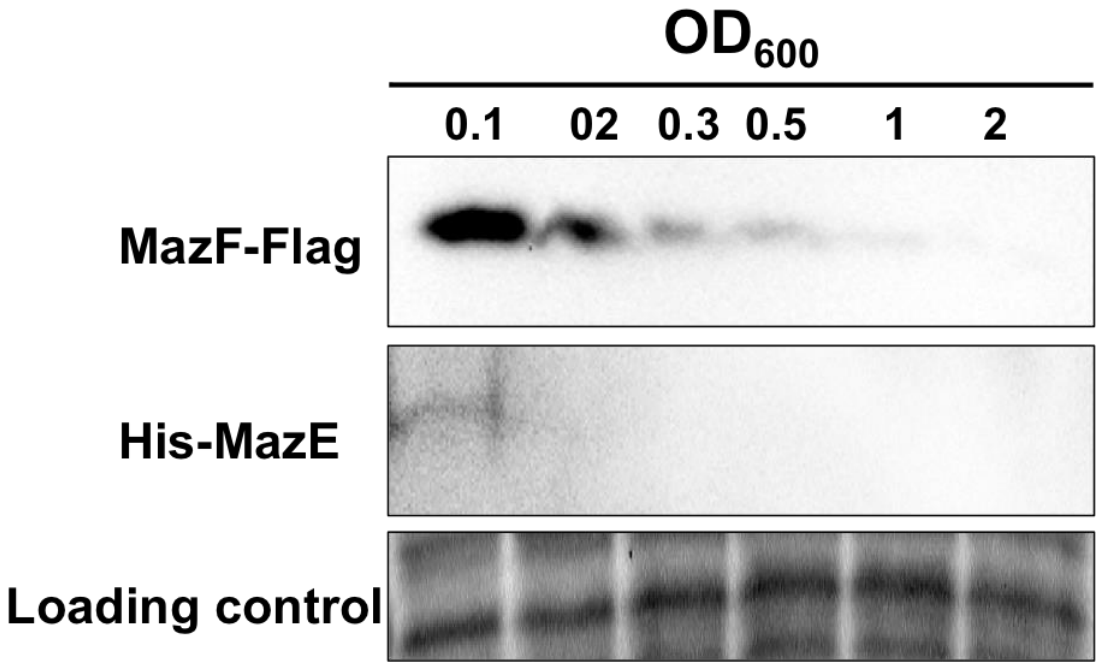

Figure 20. MazEF expression is stage dependent.

TY0807 cells harboring pUC19-p-His-*mazE-mazF*-Flag at 37°C and samples were withdrawn at indicated optical densities then samples were mixed with SB and analyzed by 20% SDS-PAGE, followed by western blotting with antibodies against His-tag for MazE detection and FLAG-tag for MazF using the lower part of the gel and the upper part of the gel was used for CBB staining to generate loading control.

IRRADIATION TIME	SURVIVAL PERCENTAGE	NO. OF SINGLE PLAQUES TESTED	NO. OF CANDIDATES
11 sec	9.40%	513	0
14 sec	3.10%	693	0
18 sec	1.20%	696	0
29 sec	0.08%	870	0
Total		**2772**	

Table 2. Search for other factors responsible for MazF inactivation.
T4Δ*alt* was irradiated with UV light for indicated times, followed by appropriate dilutions and plated on TY0901 at 37°C overnight. Single plaques were then picked by sterile toothpick and stabbed on soft agar containing TY0807 (WT) or TY0901 (Δ*mazEF*). A total of 2772 single plaques were tested for their ability to grow on TY0901 but not TY0807, no candidates were found.

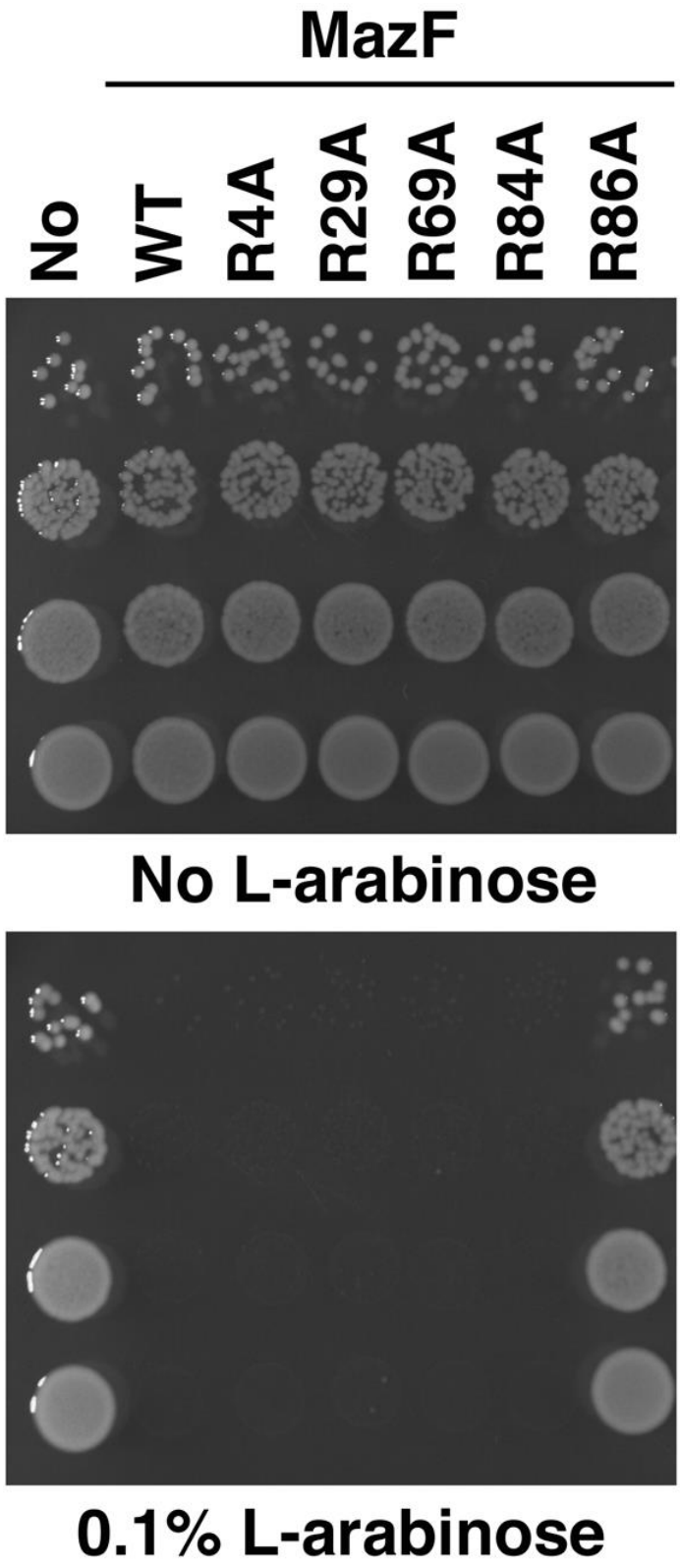

Figure 21. Effect of arginines on MazF toxicity.

An overnight culture of TY0807 cells harboring pBAD33 (No) or each plasmid expressing wild-type or designated mutants of MazF under the control of an arabinose-inducible promoter was serially 10-fold diluted. Two micro liters of each dilution were spotted onto an LB plate containing 30 μg ml^{-1} chloramphenicol with (lower panel) or without (upper panel) 0.1% L-arabinose, and incubated at 37°C overnight. An arginine at position 86 of MazF is necessary for MazF toxicity.

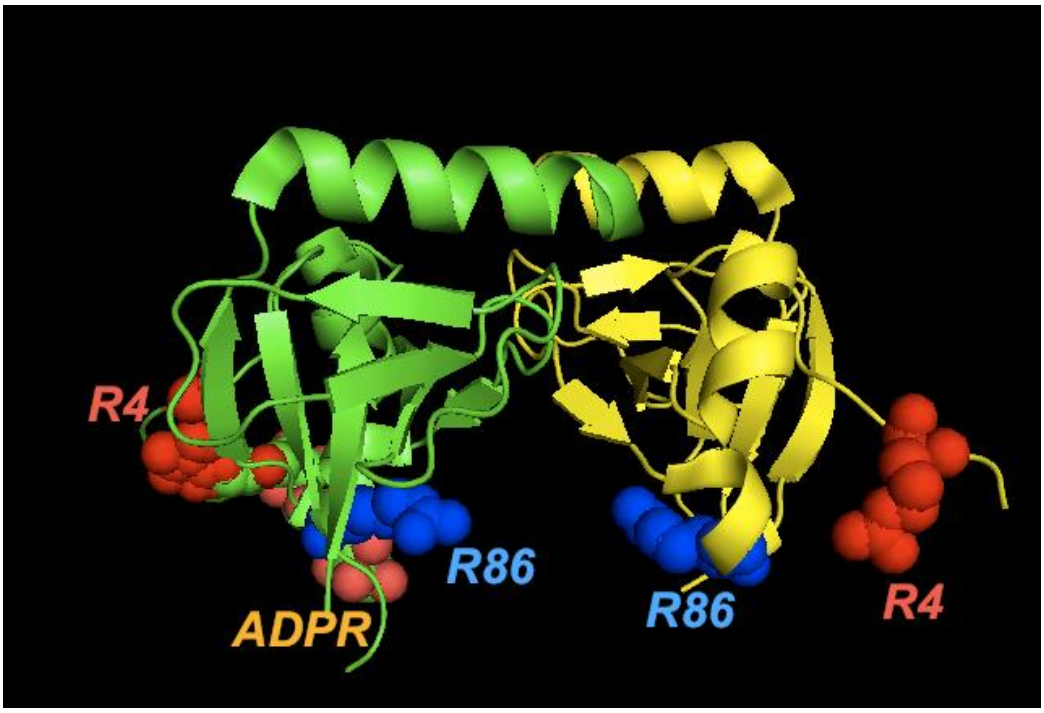

Front

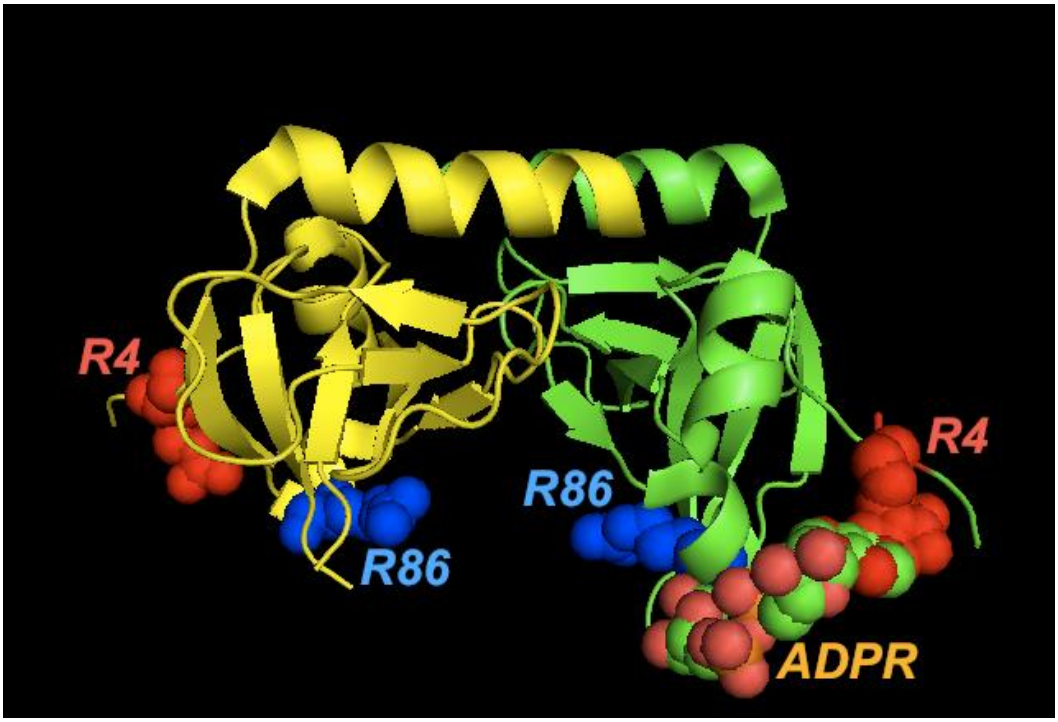

Back

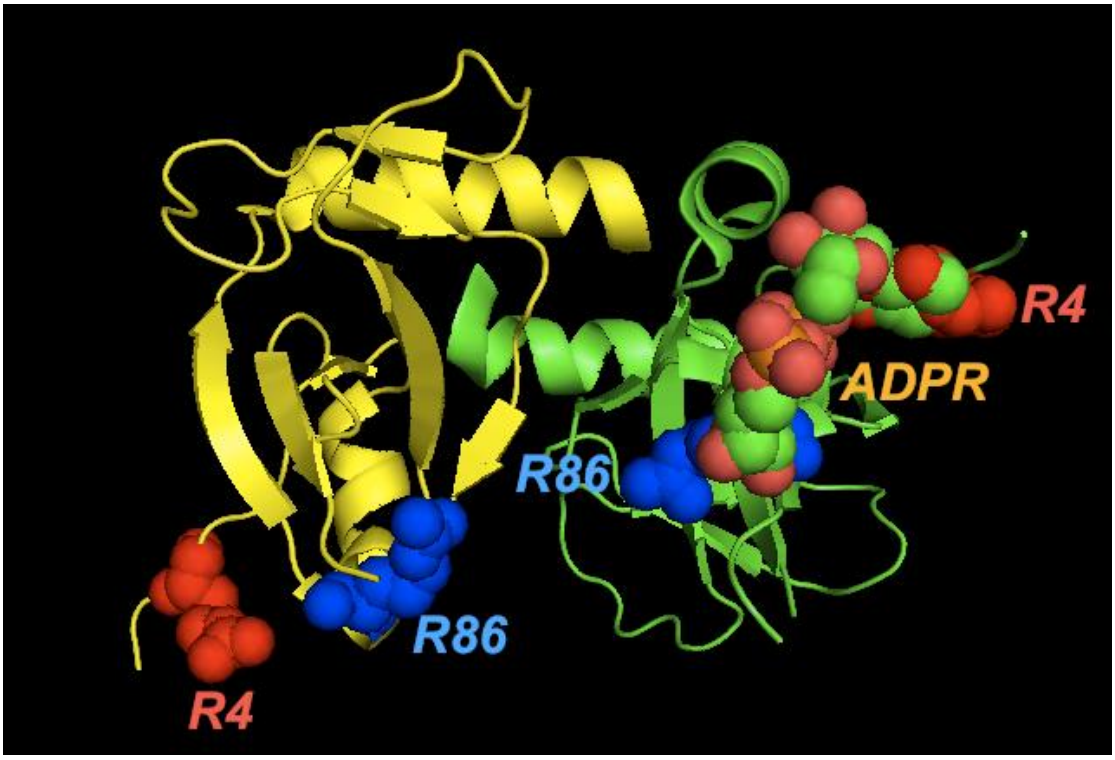

Bottom

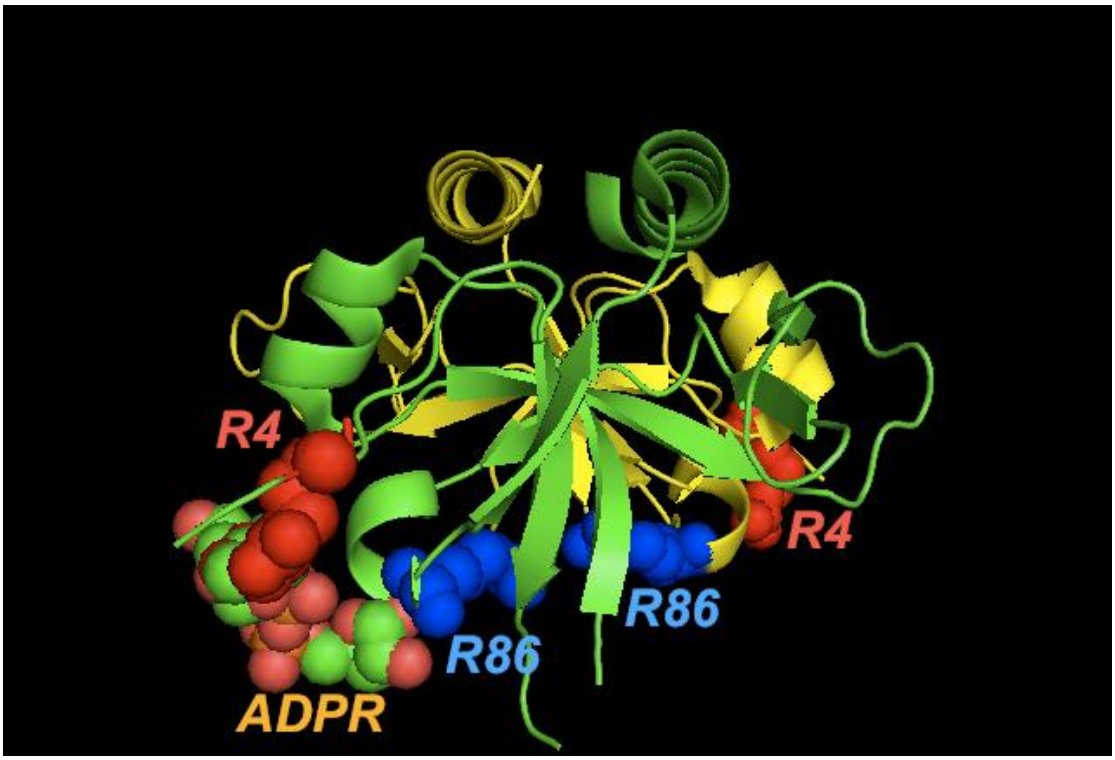

Side

Figure 22. A 3D structure of MazF dimer as reported by *Kamada et al., 2003* (PDB ID: 1UB4).

To one subunit of the MazF dimer an ADP-ribose is attached to R4. Images are generated by PyMOL. ADP-ribose might directly interact with R86 or block the active site of MazF as well as changing the positively charged side chain of R4 into a double negatively charged ADP-ribose.

Figure 23. Sequence alignment of T4 Alt and T2 Alt.

T4 Alt and T2 Alt share 70% identity.

References

Aizenman, E., Engelberg-Kulka, H., and Glaser, G. (1996) An *Escherichia coli* chromosomal “addiction module” regulated by guanosine 3′,5′-bispyrophosphate: a model for programmed bacterial cell death. *Proc Natl Acad Sci U S A* **93:** 6059-6063.

Aakre, C.D., Phung, T.N., Huang, D., and Laub, M.T. (2013) A bacterial toxin inhibits DNA replication elongation through a direct interaction with the β sliding clamp. Mol. Cell 52:617.

Amato, S.M., Orman, M.A., and Brynildsen, M.P. (2013) Metabolic control of persister formation in *Escherichia coli*. *Mol Cell* **50:** 475-487.

Amitai S, Yassin Y, Engelberg-Kulka H. (2004) MazF-mediated cell death in Escherichia coli: a point of no return. J Bacteriol. 186(24):8295-300.

Bandyopadhyay PK, Studier FW, Hamilton DL, Yuan R. (1985) Inhibition of the type I restrictionmodification enzymes EcoB and EcoK by the gene 0.3 protein of bacteriophage T7. J Mol Biol. 182:567–78.

Barrangou R, Fremaux C, Deveau H, Richards M, et al. (2007) CRISPR provides acquired resistance against viruses in prokaryotes. Science. 315:1709–12.

Bergh O, Borsheim KY, Bratbak G, Heldal M. (1989) High abundance of viruses found in aquatic environments. Nature. 340:467–8.

Bidnenko E, Ehrlich D, Chopin MC. (1995) Phage operon involved in sensitivity to the Lactococcus lactis abortive infection mechanism AbiD1. J Bacteriol. 177:3824.

Blower, T.R., Fineran, P.C., Johnson, M.J., Toth, I.K., Humphreys, D.P., and Salmond, G.P.C. (2009) Mutagenesis and functional characterization of the RNA and protein components of the *toxIN* abortive infection and toxin-antitoxin locus of *Erwinia*. *J Bacteriol* **191:** 6029-6039.

Bøggild, A.; Sofos, N.; Andersen, K.R.; Feddersen, A.; Easter, A.D.; Passmore, L.A.; Brodersen, D.E. (2012) The crystal structure of the intact E. coli RelBE toxin-antitoxin complex provides the structural basis for conditional cooperativity. Structure, 20, 1641–1648.

Buts, L., Lah, J., Dao-Thi, M-H., Wyns, L., and Loris, R. (2005) Toxin-antitoxin modules as bacterial metabolic stress managers. *Trends Biochem Sci* **30:** 672-679.

Chibani-Chennoufi S, Bruttin A, Dillmann ML, Brussow H. (2004) Phage-host interaction: an ecological perspective. J Bacteriol. 186:3677.

Corda, D., and Di Girolamo, M. (2003) Functional aspects of protein mono-ADP-ribosylation. *EMBO J* **22:** 1953-1958.

Datsenko, K.A., and Wanner, B.L. (2000) One-step inactivation of chromosomal genes in *Escherichia coli* K-12 using PCR products. *Proc Natl Acad Sci U S A* **97:** 6640-6645.

Depping, R., Lohaus, C., Meyer, H.E., and Rüger, W. (2005) The mono-ADP-ribosyltransferases Alt and ModB of bacteriophage T4: Target proteins identified. *Biochem Biophys Res Commun* **335:** 1217-1223.

Deveau H, Barrangou R, Garneau JE, Labonte J, et al. (2008) Phage response to CRISPR-encoded resistance in Streptococcus thermophilus. J Bacteriol. 190:1390–400.

Durmaz E, Klaenhammer TR. (2007) Abortive phage resistance mechanism AbiZ speeds the lysis clock to cause premature lysis of phage-infected Lactococcus lactis. J Bacteriol. 189:1417.

Dy, R.L., Przybilski, R., Semeijn, K., Salmond, G.P., and Fineran, P.C. (2014) A widespread bacteriophage abortive infection system functions through a Type IV toxin-antitoxin mechanism. *Nucleic Acids Res*. **42:** 4590-4605.

Fineran, P.C., Blower, T.R., Foulds, I.J., Humphreys, D.P., Lilley, K.S., and Salmond, G.P.C. (2009) The phage abortive infection system, ToxIN, functions as a protein-RNA toxin-antitoxin pair. *Proc Natl Acad Sci USA* **106:** 894-899.

Fozo, E.M., Makarova, K.S., Shabalina, S.A., Yutin, N., Koonin, E.V., and Storz, G. (2010) Abundance of type I toxin-antitoxin systems in bacteria: searches for new candidates and discovery of novel families. *Nucleic Acids Res* **38:** 3743-3759.

Georgiou T, Yu YTN, Ekunwe S, Buttner MJ, et al. (1998) Specific peptide-activated proteolytic cleavage of Escherichia coli elongation factor Tu. Proc Natl Acad Sci USA. 95:2891.

Gerdes, K., Christensen, S.K., and Løbner-Olesen, A. (2005) Prokaryotic toxin-antitoxin stress response loci. *Nat Rev Microbiol* **3:** 371-382.

Gerdes, K., and Wagner, E.G.H. (2007) RNA antitoxins. *Curr Opin Microbiol* **10:** 117-124.

Germain, E., Castro-Roa, D., Zenkin, N., and Gerdes, K. (2013) Molecular mechanism of bacterial persistence by HipA. *Mol Cell* **52:** 248-254.

Gotfredsen, M.; Gerdes, K. (1998) The Escherichia coli relBE genes belong to a new toxin-antitoxin gene family. Mol. Microbiol., 29, 1065–1076.

Gerdes K, Christensen SK, Løbner-Olesen A. (2005) Prokaryotic toxin-antitoxin stress response loci. Nat Rev Microbiol. 3(5):371-82.

Guzman, L.M., Belin, D., Carson, M.J., and Beckwith, J. (1995) Tight

Regulation, Modulation, and High-Level Expression by Vectors Containing the Arabinose P_{BAD} Promoter. *J Bacteriol* **177:** 4121-4130.

Hazan, R., and Engelberg-Kulka, H. (2004) *Escherichia coli mazEF*-mediated cell death as a defense mechanism that inhibits the spread of phage P1. *Mol Genet Genomics* **272:** 227-234.

Heidelberg JF, Nelson WC, Schoenfeld T, Bhaya D. (2009) Germ warfare in a microbial mat community: CRISPRs provide insights into the co-evolution of host and viral genomes. PLoS One. 4:e4169.

Homyk, T.Jr., and Weil, J. (1974) Deletion analysis of two nonessential regions of the T4 genome. *Virology* **61:** 505-523.

Hu, Y., Benedik, M.J., and Wood, T.K. (2012) Antitoxin DinJ influences the general stress response through transcript stabilizer CspE. *Environ Microbiol* **14:** 669-679.

Ishino Y, Shinagawa H, Makino K, Amemura M, et al. (1987) Nucleotide sequence of the iap gene responsible for alkaline phosphatase isozyme conversion in Escherichia coli, and identification of the gene product. J Bacteriol. 169:5429.

Itoh, T., and Tomizawa, J. (1980) Formation of an RNA primer for initiation of replication of ColE1 DNA by ribonuclease H. *Proc Natl Acad Sci USA* **77:** 2450-2454.

Jiang, Y., Pogliano, J., Helinski, D.R., and Konieczny, I. (2002) ParE toxin encoded by the broad-host-range plasmid RK2 is an inhibitor of *Escherichia coli* gyrase. *Mol Microbiol* **44:** 971-979.

Kai, T., Selick, H.E., and Yonesaki, T. (1996) Destabilization of bacteriophage T4 mRNAs by a mutation of gene *61.5*. *Genetics* **144:** 7-14.

Kamada, K., Hanaoka, F., and Burley, S.K. (2003) Crystal structure of the MazE/MazF complex: molecular bases of antidote-toxin recognition. *Mol Cell* **11:** 875-884.

Kim, Y., Wang, X., Ma, Q., Zhang, X.S., and Wood, T.K. (2009) Toxin-antitoxin systems in *Escherichia coli* influence biofilm formation through YjgK (TabA) and fimbriae. *J Bacteriol* **191:** 1258-1267.

Koga, M., Otsuka, Y., Lemire, S., and Yonesaki, T. (2011) *Escherichia coli rnlA* and *rnlB* compose a novel toxin-antitoxin systems. *Genetics* **187:** 123-130.

Kruger DH, Bickle TA. (1983) Bacteriophage survival: multiple mechanisms for avoiding the deoxyribonucleic acid restriction systems of their hosts. Microbiol Rev.; 47:345–60.

Kutter, E., White, T., Kashlev, M., Uzan, M., Mckinney, J., and Guttman, B. (1994) Effects on Host Genome Structure and Expression. In *Molecular Biology of Bacteriophage T4*. Karam, J.D., Drake, J.W., Kreuzer, K.N., Mosig, G., Hall, D.H., Eiserling, F.A., Black, L.W., Spicer, E.K., Kutter, E., Carlson, K., and Miller, E.S. (eds). Washington, D.C.: American Society for Microbiology Press, pp. 357-368.

Li, G.Y.; Zhang, Y.; Inouye, M.; Ikura, M. (2009) Inhibitory mechanism of Escherichia coli RelE-RelB toxin-antitoxin module involves a helix displacement near an mRNA interferase active site. J. Biol. Chem. 284, 14628–14636

Lieven Buts, Jurij Lah, Minh-Hoa Dao-Thi, Lode Wyns and Remy Loris. (2005) Toxin–antitoxin modules as bacterial metabolic stress managers. Trends in Bichecm Sci. 30(12): 672-9.

Maisonneuve, E., Castro-Camargo, M., and Gerdes, K. (2013) (p)ppGpp controls bacterial persistence by stochastic induction of toxin-antitoxin activity. *Cell* **154:** 1140-1150.

Maisonneuve, E., Shakespeare, L.J., Jorgensen, M.G., and Gerdes, K. (2011) Bacterial persistence by RNA endonucleases. *Proc Natl Acad Sci USA* **108:** 13206-13211.

Marianovsky , Aizenman E, Engelberg-Kulka H, Glaser G. (2001)The regulation of the Escherichia coli mazEF promoter involves an unusual alternating palindrome. J Biol Chem. 23;276(8):5975-84.

Masuda, H., Tan, Q., Awako, N., Wu, K.P., and Inouye, M. (2012) YeeU enhances the bundling of cytoskeletal polymers of MreB and FtsZ, antagonizing the CbtA (YeeV) toxicity in *Escherichia coli*. *Mol Microbiol* **84:** 979-989.

Masuda Y, Miyakawa K, Nishimura Y, Ohtsubo E. (1993) chpA and chpB, Escherichia coli chromosomal homologs of the pem locus responsible for stable maintenance of plasmid R100. J Bacteriol. 175(21):6850-6.

Miller, H.I., Riggs, A.D., and Gill, G.N. (1973) Ribonuclease H (Hybrid) in *Escherichia coli*. Identification and characterization. *J Biol Chem* **248:** 2621-2624.

Monica Markovski and Sue Wickner (2013) Preventing Bacterial Suicide: A Novel Toxin-Antitoxin Strategy. Molecular Cell 52:611-612.

Morad I, Chapman-Shimshoni D, Amitsur M, Kaufmann G. (1993) Functional expression and properties of the tRNA (Lys)-specific core anticodon nuclease encoded by Escherichia coli prrC. J Biol Chem. 268:26842.

Mutschler, H., Gebhardt, M., Shoeman, R.L., and Meinhart, A. (2011) A novel mechanism of programmed cell death in bacteria by toxin-antitoxin systems corrupts peptidoglycan synthesis. *PLoS Biol* **9:** e1001033.

Naka, K., Koga, M., Yonesaki, T., and Otsuka, Y. (2014) RNase HI stimulates the activity of RnlA toxin in *Escherichia coli*. *Mol Microbiol* **91:** 596-605.

Neubauer, C.; Gao, Y.G.; Andersen, K.R.; Dunham, C.M.; Kelley, A.C.; Hentschel, J.; Gerdes, K.; Ramakrishnan, V.; Brodersen, D.E. (2009) The structural basis for mRNA recognition and cleavage by the ribosome-dependent endonuclease RelE. Cell, **139**, 1084–1095.

Otsuka, Y., and Yonesaki, T. (2005) A novel endoribonuclease, RNase LS, in *Escherichia coli*. *Genetics* **169:** 13-20.

Otsuka, Y., and Yonesaki, T. (2012) Dmd of bacteriophage T4 functions as an antitoxin against *Escherichia coli* LsoA and RnlA toxins. *Mol Microbiol* **83:** 669-681.

Pecota, D.C., and Wood, T.K. (1996) Exclusion of T4 phage by the hok/sok killer locus from plasmid R1. *J Bacteriol* **178:** 2044-50.

Qimron U, Tabor S, Richardson CC. (2010) New Details about Bacteriophage T7-Host Interactions Microbe. 5:117–20.

Ren, D., Bedzyk, L.A., Thomas, S.M., Ye, R.W., and Wood, T.K. (2004) Gene expression in *Escherichia coli* biofilms. *Appl Microbiol Biotechnol* **64:** 515-524.

Riesenfeld CS, Schloss PD, Handelsman J. Metagenomics. (2004) genomic analysis of microbial communities. Annu Rev Genet. 38:525–52.

Rohrer, H., Zillig, W., and Mailhammer, R. (1975) ADP-ribosylation of DNA-dependent RNA polymerase of *Escherichia coli* by an NAD^+: Protein ADP-ribosyltransferase from Bacteriophage T4. *Eur J Biochem* **60:** 227-238.

Sat, B., Hazan, R., Fisher, T., Khaner, H., Glaser, G., and Engelberg-Kulka, H. (2001) Programmed cell death in *Escherichia coli*: some antibiotics can trigger *mazEF* lethality. *J Bacteriol* **183:** 2041-2045.

Sberro, H., Leavitt, A., Kiro, R., Koh, E., Peleg, Y., Qimron, U., and Sorek, R. (2013) Discovery of functional toxin/antitoxin systems in bacteria by shotgun cloning. *Mol Cell* **50:** 1-13.

Schuster C.F., and Bertram, R. (2013) Toxin-antitoxin systems are ubiquitous and versatile modulators of prokaryotic cell fate. *FEMS Microbiol Lett* **340:** 73-85.

Selick, H.E., Kreuzer, K.N., and Alberts, B.M. (1988) The Bacteriophage T4 Insertion/Substitution Vector System. *J Biol Chem* **263:** 11336-11347.

Simons, R.W., Houman, F., and Kleckner, N. (1987) Improved single and multicopy *lac*-based cloning vectors for protein and operon fusions. *Gene* **53:** 85-96.

Sommer, N., Salniene, V., Gineikiene, E., Nivinskas, R., and Rüger, W. (2000) T4 early promoter strength probed *in vivo* with unribosylated and ADP-ribosylated *Escherichia coli* RNA polymerase: a mutation analysis. *Microbiology* **146:** 2643-2653.

Tan, Q., Awano, N., and Inouye, M. (2011) Yee V is an *Escherichia coli* toxin that inhibits cell division by targeting the cytoskeleton proteins, FtsZ and MreB. *Mol Microbiol* **79:** 109-118.

Torrella F, Morita RY. (1979) Evidence by electron micrographs for a high incidence of bacteriophage particles in the waters of Yaquina Bay, oregon: ecological and taxonomical implications. Appl Environ Microbiol.

Ueno H, Yonesaki T. (2001) Recognition and specific degradation of bacteriophage T4 mRNAs. Genetics 158(1):7-17.

Van Rensburg, J.J., and Hergenrother, P.J. (2013) Detection of endogenous MazF enzyme activity in *Staphylococcus aureus*. *Anal Biochem* **443:** 81-87.

Wang, X., Kim, Y., Hong, S.H., Ma, Q., Brown, B.L., Pu, M., *et al*. (2011) Antitoxin MqsA helps mediate the bacterial general stress response. *Nat Chem Biol* **7:** 356-366.

Wang, X., Lord, D.M., Cheng, H.Y., Osbourne, D.O., Hong, S.H., Sanchez-Torres, V., *et al*. (2012) A new type V toxin-antitoxin system where mRNA for toxin GhoT is cleaved by antitoxin GhoS. *Nat Chem Biol* **8:** 855-861.

Wang Z, Mosbaugh DW. (1989) Uracil-DNA glycosylase inhibitor gene of bacteriophage PBS2 encodes a binding protein specific for uracil-DNA glycosylase. J Biol Chem. 264:1163–71.

Wang Z, Mosbaugh DW. (1988) Uracil-DNA glycosylase inhibitor of bacteriophage PBS2: cloning and effects of expression of the inhibitor gene in Escherichia coli. J Bacteriol. 170:1082–91.

Winther, K.S., and Gerdes, K. (2011) Enteric virulence associated protein VapC inhibits translation by cleavage of initiator tRNA. *Proc Natl Acad Sci USA* **108:** 7403-7407.

Wommack KE, Colwell RR. Virioplankton. (2000) viruses in aquatic ecosystems. Microbiol Mol Biol Rev. 64:69.

Yamaguchi, Y., and Inouye, M. (2009) mRNA interferases, sequence-specific endoribonucleases from the toxin-antitoxin systems. *Prog Mol Biol Transl Sci* **85:** 467-500.

Yamaguchi, Y., and Inouye, M. (2011) Regulation of growth and death in *Escherichia coli* by toxin-antitoxin systems. *Nat Rev Microbiol* **9:** 779-790.

Yarmolinsky, M.B. (1995) Programmed cell death in bacterial populations. *Science* **267:** 836-837.

Zhang, Y., and Inouye, M. (2011) RatA (YfjG), an *Escherichia coli* toxin, inhibits 70S ribosome association to block translation initiation. *Mol Microbiol* **79:** 1418-1429.

Zhang, Y., Zhang, J., Hara, H., Kato, I., and Inouye, M. (2005) Insights into the mRNA cleavage mechanism by MazF, an mRNA interferase. *J Biol Chem* **280:** 3143-3150.

Publications

Abdulraheem M. Alawneh, Dan Qi, Tetsuro Yonesaki and Yuichi Otsuka. An ADP-ribosyltransferase Alt of bacteriophage T4 negatively regulates the *Escherichia coli* MazF toxin of a toxin–antitoxin module. Mol Microbiol. 2016 Jan;99(1):188-98. doi: 10.1111/mmi.13225. Epub 2015 Oct 20.

Dan Qi, **Abdulraheem M. Alawneh**, Tetsuro Yonesaki and Yuichi Otsuka. Bacteriophage T4 Srd accelerates the degradation of Escherichia coli mRNAs via stimulating RNase E activity. GENETICS November 1, 2015 vol. 201 no. 3 977-987; DOI: 10.1534/genetics.115.180364

Acknowledgment

I would like to express my deepest gratitude and appreciation to my supervisor Prof. Tetsuro Yonesaki for supporting my research and development for more than 5 years. I am proud to have known such a great man whom I learned from more than just science, indeed my experience with Prof. Yonesaki helped me grow and will continue to do so in my future.

I also would like to thank Prof. Hiroshi Kanazawa, Prof. Hisao Masukata, Prof. Tatsuo Kakimoto and Prof. Hiroki Nishida for finding the time to advice me on the thesis until it reached its final form.

I wish to present special thanks for Dr. Yuichi Otsuka for supporting my development during my time at Prof. Yonesaki lab and sharing his experience as well as his great ideas.

I send my greetings and thanks to and Dr. Kim Kwang for helping with MS analysis.

I also would like to thank all our past and present lab members (students and secretaries) for forming such a great family and sharing their time and experiences with me.

I wish to thank the Japanese government for granting me the MEXT scholarship, without their support none of this would have been possible.

I also wish to thank the staff of the Radioisotope Research Center at Toyonaka, Osaka University, for the facilitation of our research, because all of my experiments using radioisotopes were carried out at their center.

Finally I would like to thank my family for being there for me and supporting my decision to continue my studies in Japan. I would like to apologize to them for all the hardships they went through while I am away and had no means to help. To my parents I present my achievement and I only wish they will be proud of their son.

Abdulraheem Alawneh